ACCSCIENCE PUBLISHING
An International Journal of Optimization and Control: Theories & Applications
ISSN: 2146-0957 eISSN: 2146-5703
Vol. 16, No. 2, pp.619-637 (2026)
https://doi.org/10.36922/IJOCTA025490224
IJOCTA
RESEARCH ARTICLE

A fractal–fractional differential model for distributed denial-of-service attack dynamics

Mumtaz Ali[1,2], Nazreen Waeleh[3], Nooraini Zainuddin[2*], Hanita Daud[2], and Rahimah Jusoh[4]

[1] Basic Sciences Department, Faculty of Science, Balochistan University of Engineering and Technology, Khuzdar, Balochistan, Pakistan
[2] Department of Applied Science, Faculty of Science, Management and Computing, Universiti Teknologi PETRONAS, Seri Iskandar, Perak, Malaysia
[3] Department of Electronic Engineering, Faculty of Electronics and Computer Technology and Engineering, Universiti Teknikal Malaysia Melaka, Hang Tuah Jaya, Durian Tunggal, Melaka, Malaysia
[4] Centre for Mathematical Sciences, Universiti Malaysia Pahang, Al-Sultan Abdullah, Kuantan, Pahang, Malaysia
mumtaz.ali@buetk.edu.pk, nazreen@utem.edu.my, aini_zainuddin@utp.edu.my, hanita_daud@utp.edu.my, rahimahj@umpsa.edu.my

ARTICLE INFO

Article history:
Received: December 5, 2025
Revised: December 23, 2025
Accepted: December 26, 2025
Published Online: March 17, 2026

Keywords:
Atangana–Baleanu operator
Cybersecurity modeling
Distributed denial-of-service
Existence and uniqueness
Fractal–fractional derivative
MS Classification 2010:

ABSTRACT

Distributed denial-of-service (DDoS) attacks have become a major threat to the stability of critical infrastructure networks, where even short service disruptions can lead to severe operational and economic consequences. To better capture the complex dynamics of these attacks, we extend an existing epidemic-based DDoS model by employing the fractal–fractional (FF) Atangana–Baleanu (AB) operator, which effectively accounts for memory effects, network heterogeneity, and irregular traffic patterns commonly observed in cyber environments. Within this framework, we establish the existence and uniqueness of solutions and examine the Ulam–Hyers stability of the proposed system. The local stability of both infection-free and endemic equilibria is assessed to identify the conditions under which the network can maintain normal operation. Numerical simulations are performed using the Adams–Bashforth method for various combinations of fractional and fractal orders. The results show that the FFAB formulation captures slower decay, extended memory, and more realistic transient dynamics than its classical counterpart. These findings demonstrate that incorporating FF dynamics offers a more flexible and accurate representation of DDoS propagation and quarantine-based mitigation, providing valuable insights for enhancing the resilience of modern cyber-infrastructure systems.

1. Introduction

In the modern era, the progress of nations and the well-being of societies depend largely on the security and uninterrupted operation of critical infrastructures (CIs). Power and energy systems, communication networks, transportation routes, banking and financial services, water distribution, medical facilities, industrial production, defense, and emergency response systems are examples of these infrastructures. Together, they form the essential framework that supports national development, making their reliability indispensable.[1] As information and communication technologies have advanced, many of these sectors have become increasingly interconnected and dependent on internet-based control and monitoring systems. This growing reliance has also widened the exposure of CIs to a variety of cyber risks.[2]

Contemporary cyber-attacks are capable of disrupting entire networks or targeting specific components such as supervisory control and data acquisition units, process controllers, and distributed control modules.[3] These occurrences

pose a threat to the availability, confidentiality, and integrity of vital services, and in extreme circumstances, they may escalate into more serious security crises. Due to the intricate connections between these infrastructures, a disruption in one area might spread to others and, in certain situations, even affect several nations that have similar cybersecurity policies. This has made cybersecurity a major national and worldwide concern.[4]

Distributed attacks are one of the most common types of cyber threats. A distributed denial-of-service (DDoS) attack is a notable example, where attackers compromise numerous devices, often through malware hidden in email attachments, applications, or media files, and later activate them to launch a synchronized attack on the target.[5] The increasing dependence on wireless networks has further amplified this risk, as many wireless systems lack the strong security features found in wired systems.[6] Malware spreads rapidly through daily network activity such as email communication, web browsing, software downloads, and device sharing. Similar to biological diseases, malicious code can propagate through the network and infect devices at high speed.[7] Understanding how malware spreads and how it can be stopped is essential for maintaining a secure and reliable infrastructure. Quarantine-based defense strategies, inspired by disease control, isolate highly infected nodes until they are secured, thereby preventing further spread. The success of such strategies has made them effective in mitigating large-scale threats like DDoS.[8–10]

The development of an epidemic-style mathematical model for cybersecurity has been spurred by the comparison between the spread of malware and biological epidemics. Network devices move between compartments like susceptible, infected, quarantined, and recovered under such a structure. The traditional models based on ordinary differential equations (ODEs) have proven effective for analyzing network vulnerability, stability, and threshold conditions for cyber-attack scenarios.[11]

By enabling the differentiation and integration of non-integer orders, fractional calculus (FC) expands on classical calculus. Unlike integer-order models, which typically capture only instantaneous rates of change, fractional models incorporate long-term memory and hereditary characteristics. This enables fractional systems to reflect the influence of past state on present behavior, making FC particularly suitable for modeling processes where history plays a decisive role.[12–15] Over time, many different forms of fractional derivatives have been proposed in an effort to more accurately describe systems with memory-dependent behavior.

Classical operators include the conformable derivatives,[16] Grünwald-Letnikov,[17] Caputo-Fabrizio,[18] Caputo,[19] Hadamard,[20] and Erdélyi–Kober.[21] Every derivative has unique mathematical properties that determine its suitability for specific applications. For example, the Caputo derivative offers physically meaningful initial conditions, and conformable derivatives ensure classical derivative behavior when the order approaches unity. Despite their advantages, several traditional formulations face limitations, including singular kernels, difficulties in handling physical initial constraints, and a restricted ability to capture nonlinear memory effects present in many natural phenomena. These limitations have encouraged the development of more general and flexible frameworks capable of representing complex systems more faithfully. Among these, the Atangana–Baleanu (AB) derivative has gained particular attention due to its non-singular, non-local Mittag-Leffler kernel, which provides smoother memory effects and improved stability in modeling dynamic processes.[22–24]

Further advancement came with the development of fractal–fractional (FF) operators, which combine fractional differentiation with fractal dimensions.[25] This allows the modeling of systems in which both historical dependence and irregular, non-smooth structures are present. FF models have shown strong suitability in systems such as viscoelastic materials,[26,27] environmental dynamics,[28] signal propagation, biological processes,[29–33] and other phenomena where classical or standard fractional operators may not fully capture system complexity.[34–36]

In cybersecurity research, epidemic modeling of DDoS attacks has gained traction in recent years. Zaeem et al.[37] presented an epidemic-based DDoS model in which CI nodes were categorized into susceptible, infected, quarantined, and recovered compartments. Their study utilized synthetic data, Adams numerical solvers, and nonlinear autoregressive machine learning networks to analyze the effects of seclusion strategies and understand infection, quarantine efficiency, and recovery conditions. The performance of their approach was validated through extensive simulation and convergence analysis using statistical metrics, error histograms, correlation analysis, and comparative evaluation against other back propagation learning schemes.

Similarly, Rao et al.[38] proposed a quarantine-based DDoS defense model for CI networks. Their study examined whether quarantining compro-

mised nodes could minimize malware spread and maintain network operation during active attacks. Through stability analysis at infection-free and endemic equilibria along with numerical simulations, they demonstrated that quarantine can significantly reduce attack propagation and improve system resilience. Pham et al.[39] revisited existing continuous-time DDoS models and provided a rigorous proof of global asymptotic stability for both disease-free and endemic equilibria by exploiting the cascade structure of the governing ODE systems. Their approach offers a simpler and more general framework for analyzing stability in a wide range of cyber-attack models. Although these contributions highlight the value of epidemic models in cyber-defense, the existing literature has heavily relied on classical, integer-order differential systems. Such formulations do not account for the combined effects of long-range memory and fractal irregularities that naturally arise in real network traffic. This leaves a clear gap in constructing models that more accurately capture the complex dynamics of DDoS propagation. To the best of our knowledge, no prior work has extended or modified this epidemic type DDoS model using the FFAB operator.

Motivated by these developments, the present work reformulates the DDoS epidemic model using the FFAB derivative. In this framework, we establish the existence and uniqueness of the solution, analyze Ulam–Hyers (UH) stability, and further employ the Adams–Bashforth method[40] to perform simulations for various combinations of fractional and fractal orders. This enables a more realistic and flexible representation of attack dynamics and defense mechanisms in complex cyber environments.

From a cybersecurity perspective, the fractional order component of the proposed model represents the long-term memory and persistence of DDoS attack traffic, capturing delayed mitigation effects caused by filtering latency, network congestion, and adaptive defense mechanisms. Lower fractional order values correspond to a stronger influence of past attack activity, reflecting sustained or recurring attack behaviors observed in real-world networks. The fractal component accounts for network heterogeneity and irregular traffic patterns arising from distributed botnets and non-uniform network topologies. By incorporating both effects, the proposed FF formulation provides a physically meaningful and interpretable framework for analyzing delayed responses and persistent attack dynamics, thereby enhancing its applicability to cybersecurity defense and engineering decision-making.

2. Preliminaries

This section presents the essential definitions required for the present study. These concepts form the foundation for a more detailed investigation of FFAB operators.[25]

Definition 2.1. The FF derivative of the function $y(t)$, with fractional order θ_1 and fractal order θ_2, defined in the Caputo sense with Mittag–Leffler kernel, is given as follows[25]:

$$ {}_{0}^{FFAB}D_{t}^{\theta_1,\theta_2} y(t) = \frac{\Lambda(\theta_1)}{(1-\theta_1)} \frac{d}{dt^{\theta_2}} \int_0^t y(s) \times \exp\left(-\frac{\theta_1}{1-\theta_1}(t-s)\right) ds \tag{1} $$

where $0 < \theta_1, \theta_2, \leq 1$,and $\Lambda(0) = \Lambda(1) = 1$.

Definition 2.2. The FFAB integral of $y(t)$, with fractional order θ_1 and fractal order θ_2, is given as follows25:

$$ {}_{0}^{FFAB}J_{t}^{\theta_1,\theta_2,} y(t) = \frac{\theta_1\theta_2}{\Lambda(\theta_1)\Gamma(\theta_1)} \times \int_0^t s^{\theta_2-1}(t-s)^{\theta_1-1} y(s)\, ds + \frac{\theta_2(1-\theta_1)\, t^{\theta_1-1}}{\Lambda(\theta_1)} y(t). \tag{2} $$

3. Mathematical model and basic assumptions

The node population in the suggested model is divided into two categories: the target nodes and the attacker nodes. The attacker's main objective is to identify as many vulnerable nodes as possible within its own population and use them to launch attacks on the targeted group. Any nodes impacted by a DDoS attack are cleaned, placed under quarantine, and then returned to the recovered class, as the overall number of the targeted population is considered constant. This guarantees that the target population remains unchanged. One of the two purposes of vulnerable hosts is to find other susceptible nodes. These vulnerable nodes do not achieve permanent immunity and eventually return to the susceptible class. Given that attacks on CI may be highly disruptive, the targeted network requires a significantly stronger defense mechanism.

The formulation of the epidemic model is based on the following considerations:

(i) The attacking nodes are grouped into four classes: susceptible, infected, recovered, and quarantined.

(ii) In another scenario, the attacking nodes are divided into two classes, namely, susceptible and infected.
(iii) The introduction of new nodes into the system and the natural loss of nodes not caused by attack are assumed to be minimal and are therefore represented by a constant term μ .
(iv) Both populations follow bilinear incidence, indicating that the spread of the attack is proportional to the sizes of the susceptible and infectious compartments. The infection transmission rate is β,the quarantine rate is γ, and the recovery rate is η.
(v) Recovered targeted nodes revert to the susceptible class at rate ε_t.
(vi) Infected attacking nodes return to the susceptible class at rate ε.

A complete list of model parameters and variables is provided in **Table 1**. Based on the assumptions and structure illustrated in **Figure 1**, the corresponding system of ODEs is expressed as **Equations** (3) and (4)[38]:

$$\begin{aligned}
\frac{d\mathrm{S}_t}{dt} &= -\beta \mathrm{S}_t \mathrm{I}(t) + \varepsilon_t \mathrm{R}_t, \\
\frac{d\mathrm{I}_t}{dt} &= \beta \mathrm{S}_t \mathrm{I} - \gamma \mathrm{I}_t, \\
\frac{d\mathrm{Q_t}}{dt} &= \gamma \mathrm{I}_t - \eta \mathrm{Q}_t, \\
\frac{d\mathrm{R}}{dt} &= \eta \mathrm{Q}_t - \varepsilon_t \mathrm{R}_t,
\end{aligned} \tag{3}$$

$$\begin{aligned}
\frac{d\mathrm{S}_a}{dt} &= \mu - \beta \mathrm{S}_a \mathrm{I}_a - \mu \mathrm{S}_a + \varepsilon \mathrm{I}_a, \\
\frac{d\mathrm{I}_a}{dt} &= \beta \mathrm{S}_a \mathrm{I}_a - (\mu + \varepsilon)\, \mathrm{I}_a,
\end{aligned} \tag{4}$$

where $\mathrm{S}_t + \mathrm{I}_t + \mathrm{Q}_t + \mathrm{R}_t = 1$ and $\mathrm{S}_a + \mathrm{I}_a = 1$. **Equations** (3) and (4), adapted from Rao et al.,[38] can be written mathematically as follows:

$$\begin{aligned}
\frac{d\mathrm{S}_t}{dt} &= -\beta \mathrm{S}_t \mathrm{I} + \varepsilon_t (1 - \mathrm{S}_t - \mathrm{I}_t - \mathrm{Q}_t), \\
\frac{d\mathrm{I}_t}{dt} &= \beta \mathrm{S}_t \mathrm{I} - \gamma \mathrm{I}_t, \\
\frac{d\mathrm{Q}_t}{dt} &= \gamma \mathrm{I}_t - \eta \mathrm{Q}_t, \\
\frac{d\mathrm{I}}{dt} &= \eta (1 - \mathrm{I})\, \mathrm{I} - (\mu + \varepsilon)\, \mathrm{I}.
\end{aligned} \tag{5}$$

The feasible region of **Equation** (5) can be written as $\Omega = \mathrm{S}_t, \mathrm{I}_t, \mathrm{Q}_t, \mathrm{I} \in R^4 := \{ \mathrm{S}_t > 0, \mathrm{I}_t > 0, \mathrm{Q}_t > 0, \mathrm{S}_t + \mathrm{I}_t + \mathrm{Q}_t \leq 1, \mathrm{I} \leq 1 \}$.

Using the same ICs as in the previous case, the model is extended by replacing the classical integer-order derivative **Equation** (5) with the FFAB derivative:

$$\begin{aligned}
{}_0^{FFAB}D_t^{\vartheta,\theta}\mathrm{S}_t &= -\beta \mathrm{S}_t \mathrm{I} + \varepsilon_t (1 - \mathrm{S}_t - \mathrm{I}_t - \mathrm{Q}_t), \\
{}_0^{FFAB}D_t^{\vartheta,\theta}\mathrm{I}_t &= \beta \mathrm{S}_t \mathrm{I} - \gamma \mathrm{I}_t, \\
{}_0^{FFAB}D_t^{\vartheta,\theta}\mathrm{Q}_t &= \gamma \mathrm{I}_t - \eta \mathrm{Q}_t, \\
{}_0^{FFAB}D_t^{\vartheta,\theta}\mathrm{I} &= \eta (1 - \mathrm{I})\, \mathrm{I} - (\mu + \varepsilon)\, \mathrm{I}.
\end{aligned} \tag{6}$$

The corresponding initial conditions (ICs) associated with the above model are given as follows:

$$\mathrm{S}_t(0) = \mathrm{S}_{t0},\ \mathrm{I}_t(0) = \mathrm{I}_{t0}, \mathrm{Q}_t(0) = \mathrm{Q}_{t0},\ \mathrm{I}(0) = \mathrm{I}_0. \tag{7}$$

3.1. Positivity of solutions

Theorem 3.1. For non-negative ICs $\mathrm{S}_t(0)$, $\mathrm{I}_t(0), \mathrm{Q}_t(0)$, and $\mathrm{I}(0) \geq 0$, the solution of **Equation** (6) remains non-negative for all $t \geq 0$.

Proof. We make use of the generalized mean value theorem associated with the FF model derivative.

$$\begin{aligned}
{}_0^{FFAB}D_t^{\theta_1,\theta_2}\mathrm{S_t}\,|_{\mathrm{S}_t=0} &= \varepsilon_t (1 - \mathrm{I}_t - \mathrm{Q}_t) \geq 0, \\
{}_0^{FFAB}D_t^{\theta_1,\theta_2}\mathrm{I_t}\,|_{\mathrm{I}_t=0} &= \beta \mathrm{S}_t \mathrm{I} \geq 0, \\
{}_0^{FFAB}D_t^{\theta_1,\theta_2}\mathrm{Q_t}\,|_{\mathrm{Q}_t=0} &= \gamma \mathrm{I}_t \geq 0, \\
{}_0^{FFAB}D_t^{\theta_1,\theta_2}\mathrm{I}\,|_{\mathrm{I}=0} &= 0.
\end{aligned} \tag{8}$$

The non-negativity of the derivative at the boundaries of all compartments ensures that the solutions remain non-negative for all $t \geq 0$.

3.2. Existence and uniqueness analysis

We now turn to the fundamental analytical results concerning the existence and uniqueness of solutions to **Equation** (6). These results are obtained using a fixed-point framework. The existence and uniqueness of the solution to **Equation** (8) are established using the FFM framework. For clarity, the e-epidemic DDoS model is formulated as follows:

$$\begin{aligned}
{}_0^{FFAB}D_t^{\theta_1,\theta_2}\mathrm{S}_t &= \Xi_1(t, \mathrm{S_t}), \\
{}_0^{FFAB}D_t^{\theta_1,\theta_2}\mathrm{I}_t &= \Xi_2(t, \mathrm{I_t}), \\
{}_0^{FFAB}D_t^{\theta_1,\theta_2}\mathrm{Q}_t &= \Xi_3(t, \mathrm{Q_t}), \\
{}_0^{FFAB}D_t^{\theta_1,\theta_2}\mathrm{I} &= \Xi_4(t, \mathrm{I}).
\end{aligned} \tag{9}$$

Table 1. Nomenclature

Symbol	Description
S	Nodes that are vulnerable to attack
I	Nodes that are currently carrying out the attack
S_t	Target nodes that are susceptible to infection
I_t	Target nodes that have been infected
Q_t	Target nodes placed under quarantine
R_t	Targeted nodes that have been recovered
β	Infection transmission rate per contact
μ	Natural rate of increase and loss within the attacking node population
ε	Transition rate at which infected attacking nodes return to the susceptible class
ε_t	Rate describing how recovered targeted nodes become susceptible once more
γ	Rate at which infected attacking nodes are shifted into the quarantine group
η	Transition rate representing the movement of quarantined nodes into the recovered class after treatment

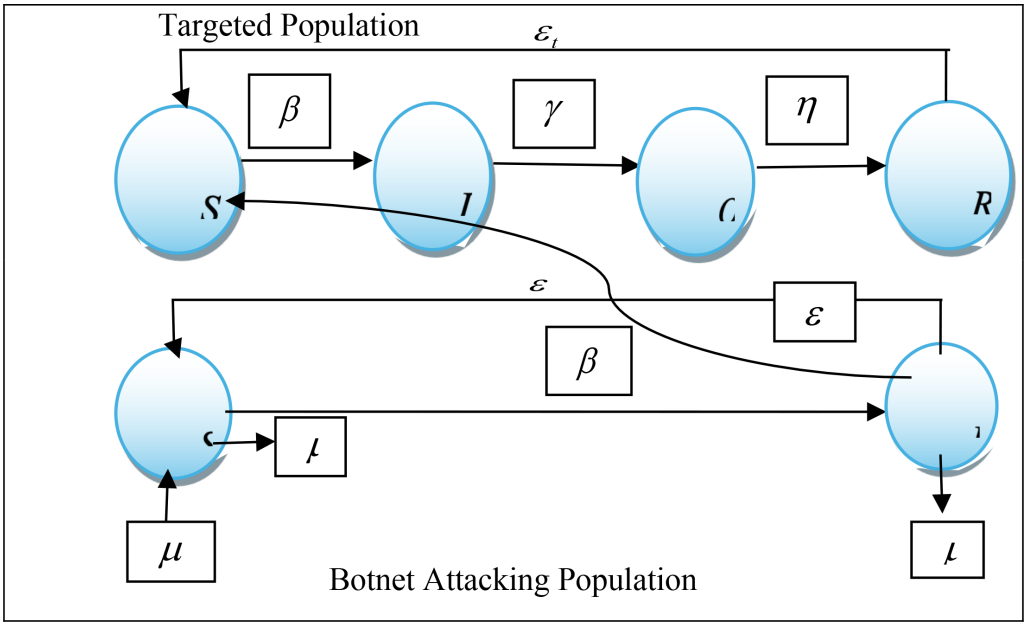

Figure 1. Schematic representation of the distributed denial-of-service attack model [38]

where:

$$\begin{aligned}
\Xi_1(t, S_t) &= -\beta S_t I + \varepsilon_t (1 - S_t - I_t - Q_t), \\
\Xi_2(t, I_t) &= \beta S_t I - \gamma I_t, \\
\Xi_3(t, Q_t) &= \gamma I_t - \eta Q_t, \\
\Xi_4(t, I) &= \eta (1 - I) I - (\mu + \varepsilon) I.
\end{aligned} \tag{10}$$

Utilizing the FFAB integral operator given in **Equation** (2), **Equation** (6) reduces to a Volterra integral type of order $0 < \theta_1, \theta_2 \leq 1$given by:

$$\begin{aligned}
S_t &= S_t(0) + \frac{\theta_2(1-\theta_1)t^{\theta_2-1}}{\Lambda(\theta_1)}\Xi_1(t, S_t) + \frac{\theta_1\theta_2}{\Lambda(\theta_1)\Gamma(\theta_1)} \\
&\times \int_0^t s^{\theta_2-1}(t-s)^{\theta_1-1}\Xi_1(s, S_t)\, ds, \\
I_t &= I_t(0) + \frac{\theta_2(1-\theta_1)t^{\theta_2-1}}{\Lambda(\theta_1)}\Xi_2(t, I_t) + \frac{\theta_1\theta_2}{\Lambda(\theta_1)\Gamma(\theta_1)} \\
&\times \int_0^t s^{\theta_2-1}(t-s)^{\theta_1-1}\Xi_2(s, I_t)\, ds, \\
Q_t &= Q_t(0) + \frac{\theta_2(1-\theta_1)t^{\theta_2-1}}{\Lambda(\theta_1)}\Xi_3(t, Q_t) + \frac{\theta_1\theta_2}{\Lambda(\theta_1)\Gamma(\theta_1)} \\
&\times \int_0^t s^{\theta_2-1}(t-s)^{\theta_1-1}\Xi_3(s, Q_t)\, ds, \\
I &= I(0) + \frac{\theta_2(1-\theta_1)t^{\theta_2-1}}{\Lambda(\theta_1)}\Xi_4(t, I) + \frac{\theta_1\theta_2}{\Lambda(\theta_1)\Gamma(\theta_1)} \\
&\times \int_0^t s^{\theta_2-1}(t-s)^{\theta_1-1}\Xi_4(s, I)\, ds.
\end{aligned} \tag{11}$$

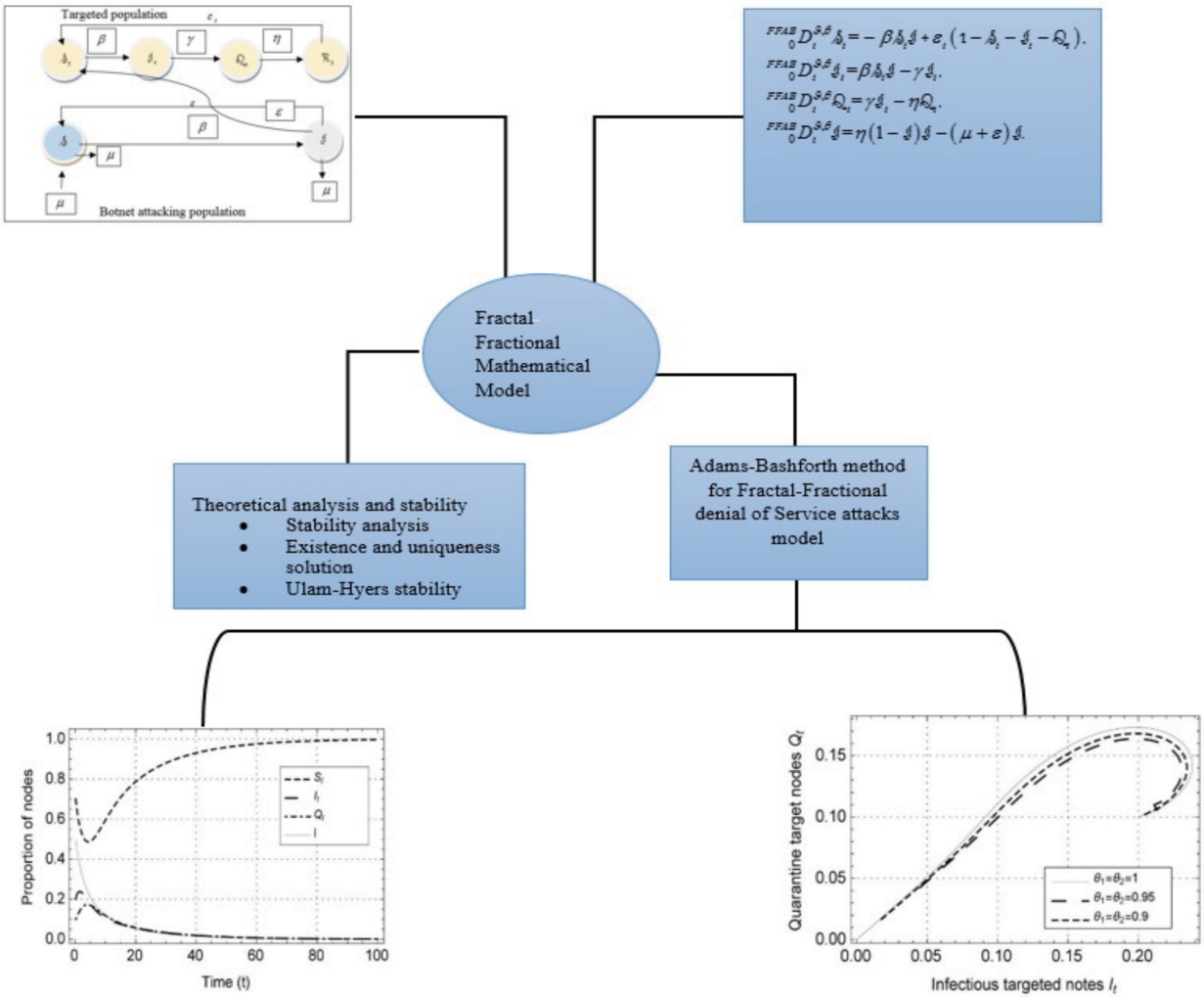

Figure 2. Schematic workflow of the fractal–fractional Atangana–Baleanu distributed denial-of-service model

(H) :For establishing our results, we impose the following conditions: Assume thatS_t, $\tilde{S}_t, I_t$, $\tilde{I}_t, Q_t$, $\tilde{Q}_t$and I, $\tilde{I}$ are continuous functions satisfying the bounds, $\|S_t\| \leq \rho_1$, $\|I_t\| \leq \rho_2, \|Q_t\| \leq \rho_3and\|I\| \leq \rho_4$, where $\rho_1, \rho_2, \rho_3,$ and $\rho_4 > 0$.

Theorem 3.2. Suppose that the inequality $0 \leq \beta\rho_4 + \varepsilon_t, < 1$ is satisfied. Then, the kernel Ξ_1 adheres to the Lipschitz condition and constitutes a contraction mapping.

Proof. For S_t and$\tilde{S}_t$, we obtain:

$$\begin{aligned}
&\left\|\Xi_1(t,S_t)-\Xi_1\left(t,\tilde{S}_t\right)\right\| \\
&=\left\|-\beta S_t I+\varepsilon_t(1-S_t-I_t-Q_t)\right. \\
&\left.+\beta\tilde{S}_t I-\varepsilon_t\left(1-\tilde{S}_t-I_t-Q_t\right)\right\|, \\
&\leq(\beta\|I\|+\varepsilon_t)\left\|S_t-\tilde{S}_t\right\|, \\
&\leq(\beta\rho_4+\varepsilon_t)\left\|S_t-\tilde{S}_t\right\|. \qquad (12)
\end{aligned}$$

Using assumption (H)and taking $L_1 = \beta\rho_4 + \varepsilon_t$,then we have:

$$\left\|\Xi_1(t,S_t)-\Xi_1\left(t,\tilde{S}_t\right)\right\| \leq L_1\left\|S_t-\tilde{S}_t\right\|. \qquad (13)$$

Hence, the Lipschitz condition L_1 is satisfied for the kernel $?_1$. In addition, the inequality $0 \leq \beta\rho_4 + \varepsilon_t < 1$ shows that $\Xi_1$is a contraction mapping. In a similar manner, it can be shown that L_2 satisfies the Lipschitz condition for I_t and$\tilde{I}_t$. Then, we obtain:

$$\begin{aligned}
\left\|\Xi_2(t,I_t)-\Xi_2\left(t,\tilde{I}_t\right)\right\| &= \|\beta S_t I-\gamma I_t\ -\beta S_t I+\gamma\tilde{I}_t\|, \\
&\leq -\gamma\left\|I_t\ -\tilde{I}_t\right\|, \qquad (14)
\end{aligned}$$

By selecting $L_2 = -\gamma$, then we get:

$$\left\|\Xi_2(t,I_t)-\Xi_2\left(t,\tilde{I}_t\right)\right\| \leq L_2\left\|I_t-\tilde{I}_t\right\|. \qquad (15)$$

We next verify that the operator L_3 satisfies the Lipschitz condition for Q_t and$\tilde{Q}_t$. Then, we

obtain:

$$\begin{aligned}&\left\|\Xi_3\left(t,\mathrm{Q}_t\right)-\Xi_3\left(t,\tilde{\mathrm{Q}}_t\right)\right\|\\&=\left\|\gamma\mathrm{I}_t-\eta\mathrm{Q}_t\ -\gamma\mathrm{I}_t+\eta\tilde{\mathrm{Q}}_t\right\|,\\&\leq\eta\left\|\mathrm{Q}_t\ -\tilde{\mathrm{Q}}_t\right\|,\end{aligned}\tag{16}$$

By choosing $L_3=\eta$, then we get:

$$\left\|\Xi_3\left(t,\mathrm{Q_t}\right)-\Xi_3\left(t,\tilde{\mathrm{Q}}_t\right)\right\|\leq L_3\left\|\mathrm{Q}_t-\tilde{\mathrm{Q}}_t\right\|.\tag{17}$$

Finally, we show that the operator L_4 satisfies the Lipschitz condition for I and$\tilde{\mathrm{I}}$ as follows:

$$\begin{aligned}&\left\|\Xi_4\left(t,\mathrm{I}\right)-\Xi_4\left(t,\tilde{\mathrm{I}}\right)\right\|=\left\|\eta\left(1-\mathrm{I}\right)\mathrm{I}-\left(\mu+\varepsilon\right)\mathrm{I}\right.\\&\left.-\eta\left(1-\tilde{\mathrm{I}}\right)\tilde{\mathrm{I}}+\left(\mu+\varepsilon\right)\tilde{\mathrm{I}}\right\|,\\&=\left\|\eta\left(\mathrm{I}-\tilde{\mathrm{I}}\right)-\mu\left(\mathrm{I}-\tilde{\mathrm{I}}\right)-\varepsilon\left(\mathrm{I}-\tilde{\mathrm{I}}\right)\right.\\&\left.-\eta\left(\mathrm{I}-\tilde{\mathrm{I}}\right)\left(\mathrm{I}-\tilde{\mathrm{I}}\right)\right\|,\\&\leq\left|\left(\eta-\mu-\varepsilon\right)-\eta\left(\mathrm{I}+\tilde{\mathrm{I}}\right)\right|\left\|\mathrm{I}-\tilde{\mathrm{I}}\right\|,\\&\leq-\left(\mu+\varepsilon\right)\left\|\mathrm{I}-\tilde{\mathrm{I}}\right\|,\end{aligned}\tag{18}$$

By choosing $L_4=-\left(\mu+\varepsilon\right)$, then we get:

$$\left\|\Xi_4\left(t,\mathrm{I}\right)-\Xi_4\left(t,\tilde{\mathrm{I}}_t\right)\right\|\leq L_4\left\|\mathrm{I}-\tilde{\mathrm{I}}\right\|.\tag{19}$$

Consequently, the operatorsΞ_1, Ξ_2, Ξ_3, and $\Xi_4$satisfy the Lipschitz condition and exhibit the contraction property.

Now, from **Equation** (10), we have

$$\begin{aligned}&\mathrm{S}_t=\mathrm{S}_t\left(0\right)+\frac{\theta_2(1-\theta_1)t^{\theta_2-1}}{\Lambda(\theta_1)}\Xi_1\left(t,\mathrm{S}_t\right)+\frac{\theta_1\theta_2}{\Lambda(\theta_1)\Gamma(\theta_1)}\\&\int_0^t s^{\theta_2-1}\left(\mathrm{t}-s\right)^{\theta_1-1}\Xi_1\left(s,\mathrm{S}_t\right)ds,\\&\mathrm{I}_t=\mathrm{I}_t\left(0\right)+\frac{\theta_2(1-\theta_1)t^{\theta_2-1}}{\Lambda(\theta_1)}\Xi_2\left(t,\mathrm{I}_t\right)+\frac{\theta_1\theta_2}{\Lambda(\theta_1)\Gamma(\theta_1)}\\&\int_0^t s^{\theta_2-1}\left(\mathrm{t}-s\right)^{\theta_1-1}\Xi_2\left(s,\mathrm{I}_t\right)ds,\\&\mathrm{Q}_t=\mathrm{Q}_t\left(0\right)+\frac{\theta_2(1-\theta_1)t^{\theta_2-1}}{\Lambda(\theta_1)}\Xi_3\left(t,\mathrm{Q}_t\right)+\frac{\theta_1\theta_2}{\Lambda(\theta_1)\Gamma(\theta_1)}\\&\int_0^t s^{\theta_2-1}\left(\mathrm{t}-s\right)^{\theta_1-1}\Xi_3\left(s,\mathrm{Q}_t\right)ds,\\&\mathrm{I}=\mathrm{I}\left(0\right)+\frac{\theta_2(1-\theta_1)t^{\theta_2-1}}{\Lambda(\theta_1)}\Xi_4\left(t,\mathrm{I}\right)+\frac{\theta_1\theta_2}{\Lambda(\theta_1)\Gamma(\theta_1)}\\&\int_0^t s^{\theta_2-1}\left(\mathrm{t}-s\right)^{\theta_1-1}\Xi_4\left(s,\mathrm{I}\right)ds,\end{aligned}\tag{20}$$

with ICs, $\mathrm{S}_t\left(0\right)=\mathrm{S}_{t0},\ \mathrm{I}_t\left(0\right)=\mathrm{I}_{t0},\mathrm{Q}_t\left(0\right)=\mathrm{Q}_{t0},\ \mathrm{I}\left(0\right)=\mathrm{I}_0$.

Our focus is now turned to the following recursive expression:

$$\begin{aligned}&\mathrm{S}_{t(\iota)}=\mathrm{S}_t\left(0\right)+\frac{\theta_2(1-\theta_1)t^{\theta_2-1}}{\Lambda(\theta_1)}\Xi_1\left(t,\mathrm{S}_{t(\iota-1)}\right)\\&+\frac{\theta_1\theta_2}{\Lambda(\theta_1)\Gamma(\theta_1)}\int_0^t s^{\theta_2-1}\left(\mathrm{t}-s\right)^{\theta_1-1}\Xi_1\left(s,\mathrm{S}_{t(\iota-1)}\right)ds,\\&\mathrm{I}_{t(\iota)}=\mathrm{I}_t\left(0\right)+\frac{\theta_2(1-\theta_1)t^{\theta_2-1}}{\Lambda(\theta_1)}\Xi_2\left(t,\mathrm{I}_{t(\iota-1)}\right)\\&+\frac{\theta_1\theta_2}{\Lambda(\theta_1)\Gamma(\theta_1)}\int_0^t s^{\theta_2-1}\left(\mathrm{t}-s\right)^{\theta_1-1}\Xi_2\left(s,\mathrm{I}_{t(\iota-1)}\right)ds,\\&\mathrm{Q}_{t(\iota)}=\mathrm{Q}_t\left(0\right)+\frac{\theta_2(1-\theta_1)t^{\theta_2-1}}{\Lambda(\theta_1)}\Xi_3\left(t,\mathrm{Q}_{t(\iota-1)}\right)\\&+\frac{\theta_1\theta_2}{\Lambda(\theta_1)\Gamma(\theta_1)}\int_0^t s^{\theta_2-1}\left(\mathrm{t}-s\right)^{\theta_1-1}\Xi_3\left(s,\mathrm{Q}_{t(\iota-1)}\right)ds,\\&\mathrm{I}_{(\iota)}=\mathrm{I}\left(0\right)+\frac{\theta_2(1-\theta_1)t^{\theta_2-1}}{\Lambda(\theta_1)}\Xi_4\left(t,\mathrm{I}_{(\iota-1)}\right)\\&+\frac{\theta_1\theta_2}{\Lambda(\theta_1)\Gamma(\theta_1)}\int_0^t s^{\theta_2-1}\left(\mathrm{t}-s\right)^{\theta_1-1}\Xi_4\left(s,\mathrm{I}_{(\iota-1)}\right)ds.\end{aligned}\tag{21}$$

Theorem 3.3. Consider the epidemic model-based DDoS attack with FFAB. If $\max\left\{L_1,L_2,L_3,L_4\right\}<1$, then the model admits at least one solution.

Proof. Let

$$\begin{aligned}&\mathrm{W}_{1\iota}=\mathrm{S}_{t(\iota+1)}-\mathrm{S}_t,\\&\mathrm{W}_{2\iota}=\mathrm{I}_{t(\iota+1)}-\mathrm{I}_t,\\&\mathrm{W}_{3\iota}=\mathrm{Q}_{t(\iota+1)}-\mathrm{Q}_t,\\&\mathrm{W}_{4\iota}=\mathrm{I}_{(\iota+1)}-\mathrm{I}.\end{aligned}\tag{22}$$

Then, we have,

$$\|\mathrm{W}_{1\iota}(t)\| = \left\|\mathrm{S}_{t(\iota+1)} - \mathrm{S}_t\right\|$$

$$= \left\| \frac{\theta_2(1-\theta_1)t^{\theta_2-1}}{\Lambda(\theta_2)} \left(\Xi_1\left(t, \mathrm{S}_{t(\iota)}\right) - \Xi_1\left(t, \mathrm{S}_t\right)\right) + \frac{\theta_1\theta_2}{\Lambda(\theta_1)\Gamma(\theta_1)} \int_0^t s^{\theta_2-1}(t-s)^{\vartheta-1} \left(\Xi_1\left(t, \mathrm{S}_{t(\iota)}\right) - \Xi_1\left(t, \mathrm{S}_t\right)\right) ds \right\|,$$

$$\leq \frac{\theta_2(1-\theta_1)t^{\theta_2-1}}{\Lambda(\theta_2)} \left\|\Xi_1\left(t, \mathrm{S}_{t(\iota)}\right) - \Xi_1\left(t, \mathrm{S}_t\right)\right\| + \frac{\theta_1\theta_2}{\Lambda(\theta_1)\Gamma(\theta_1)} \int_0^t s^{\theta_2-1}(t-s)^{\theta_1-1} \left\|\Xi_1\left(t, \mathrm{S}_{t(\iota)}\right) - \Xi_1\left(t, \mathrm{S}_t\right)\right\| ds,$$

$$\leq \frac{\theta_2(1-\theta_1)t^{\theta_2-1}}{\Lambda(\theta_1)} L_1 \left\|\mathrm{S}_{\mathrm{t}} - \tilde{\mathrm{S}}_{\mathrm{t}}\right\| + \frac{\theta_1\theta_2}{\Lambda(\theta_1)\Gamma(\theta_1)} \int_0^t s^{\theta_2-1}(t-s)^{\theta_1-1} L_1 \left\|\mathrm{S}_t - \tilde{\mathrm{S}}_t\right\| ds,$$

$$\leq \left(\frac{\theta_2(1-\theta_1)t^{\theta_2-1}}{\Lambda(\theta_1)} + \frac{\theta_1\theta_2}{\Lambda(\theta_1)\Gamma(\theta_1)} \int_0^t s^{\theta_2-1}(t-s)^{\theta_1-1} ds\right) L_1 \left\|\mathrm{S}_t - \tilde{\mathrm{S}}_t\right\|,$$

$$\leq \left(\frac{\theta_2(1-\theta_1)t^{\theta_2-1}}{\Lambda(\theta_1)} + \frac{\theta_1\Gamma(\theta_2+1)t^{\theta_1+\theta_2-1}}{\Lambda(\theta_1)\Gamma(\theta_1+\theta_2+1)}\right) L_1 \left\|\mathrm{S}_t - \tilde{\mathrm{S}}_t\right\|,$$

$$\leq \left(\frac{\theta_2(1-\theta_1)t^{\theta_2-1}}{\Lambda(\theta_1)} + \frac{\theta_1\Gamma(\theta_2+1)t^{\theta_1+\theta_2-1}}{\Lambda(\theta_1)\Gamma(\theta_1+\theta_2+1)}\right)^{\iota} L_1^{\iota} \left\|\mathrm{S}_{\mathrm{t}} - \tilde{\mathrm{S}}_{\mathrm{t}}\right\|. \tag{23}$$

Since $L_1 < 1$. As $\iota \to \infty$, then we have $\mathrm{S}_{\mathrm{t}} \to \tilde{\mathrm{S}}_{\mathrm{t}}$. In a similar manner,

$$\|\mathrm{W}_{2\iota}\| \leq \left(\frac{\theta(1-\vartheta)\mathrm{t}^{\theta-1}}{\Lambda(\vartheta)} + \frac{\vartheta\Gamma(\theta+1)\mathrm{t}^{\vartheta+\theta-1}}{\Lambda(\vartheta)\Gamma(\vartheta+\theta+1)}\right)^{\iota} L_2^{\iota} \left\|\mathrm{I}_{\mathrm{t}} - \tilde{\mathrm{I}}_{\mathrm{t}}\right\|,$$

$$\|\mathrm{W}_{3\iota}\| \leq \left(\frac{\theta(1-\vartheta)\mathrm{t}^{\theta-1}}{\Lambda(\vartheta)} + \frac{\vartheta\Gamma(\theta+1)\mathrm{t}^{\vartheta+\theta-1}}{\Lambda(\vartheta)\Gamma(\vartheta+\theta+1)}\right)^{\iota} L_3^{\iota} \left\|\mathrm{Q}_{\mathrm{t}} - \tilde{\mathrm{Q}}_{\mathrm{t}}\right\|,$$

$$\|\mathrm{W}_{4\iota}\| \leq \left(\frac{\theta(1-\vartheta)\mathrm{t}^{\theta-1}}{\Lambda(\vartheta)} + \frac{\vartheta\Gamma(\theta+1)\mathrm{t}^{\vartheta+\theta-1}}{\Lambda(\vartheta)\Gamma(\vartheta+\theta+1)}\right)^{\iota} L_4^{\iota} \left\|\mathrm{I}_{\mathrm{t}} - \tilde{\mathrm{I}}_{\mathrm{t}} S\right\|. \tag{24}$$

As $\iota \to \infty$, then we obtain $\mathrm{W}_{t\iota}(\mathrm{t}) \to 0$, with L_2, L_3 and $L_4 < 1$. Hence, **Equation** (6) admits at least one solution.

Theorem 3.4. The epidemic model-based DDoS attack with FFAB has a unique solution if

$$\left(\frac{\theta_2(1-\theta_1)t^{\theta_2-1}}{\Lambda(\theta_1)} + \frac{\theta_1\Gamma(\theta_2+1)t^{\theta_1+\theta_2-1}}{\Lambda(\theta_1)\Gamma(\theta_1+\theta_2+1)}\right) \quad L_i < 1 \text{ for } i = 1, 2, 3, 4. \tag{25}$$

Proof. Let $\tilde{\mathrm{S}}_t, \tilde{\mathrm{I}}_t, \tilde{\mathrm{Q}}_t$, and $\tilde{\mathrm{I}}$be another solution of **Equation** (6) that satisfies the same ICs as $\mathrm{S}_t, \mathrm{I}_t, \mathrm{Q}_t$, and I such that

$$\tilde{\mathrm{S}}_t = \tilde{\mathrm{S}}_t(0) + \frac{\theta_2(1-\theta_1)t^{\theta_2-1}}{\Lambda(\theta_1)}\Xi_1\left(t, \tilde{\mathrm{S}}_{\mathrm{t}}\right) + \frac{\theta_2\theta_1}{\Lambda(\theta_1)\Gamma(\theta_1)} \int_0^t s^{\theta_2-1}(t-s)^{\theta_1-1}\Xi_1\left(s, \tilde{\mathrm{S}}_{\mathrm{t}}\right) ds,$$

$$\tilde{\mathrm{I}}_{\mathrm{t}} = \tilde{\mathrm{I}}_{\mathrm{t}}(0) + \frac{\theta_2(1-\theta_1)t^{\theta_2-1}}{\Lambda(\theta_1)}\Xi_2\left(t, \tilde{\mathrm{I}}_{\mathrm{t}}\right) + \frac{\theta_2\theta_1}{\Lambda(\theta_1)\Gamma(\theta_1)} \int_0^t s^{\theta_2-1}(t-s)^{\theta_1-1}\Xi_2\left(s, \tilde{\mathrm{I}}_{\mathrm{t}}\right) ds,$$

$$\tilde{\mathrm{Q}}_{\mathrm{t}} = \tilde{\mathrm{Q}}_{\mathrm{t}}(0) + \frac{\theta_2(1-\theta_1)t^{\theta_2-1}}{\Lambda(\theta_1)}\Xi_3\left(t, \tilde{\mathrm{Q}}_{\mathrm{t}}\right) + \frac{\theta_2\theta_1}{\Lambda(\theta_1)\Gamma(\theta_1)} \int_0^t s^{\theta_2-1}(t-s)^{\theta_1-1}\Xi_3\left(s, \tilde{\mathrm{Q}}_{\mathrm{t}}\right) ds,$$

$$\tilde{\mathrm{I}} = \tilde{\mathrm{I}}(0) + \frac{\theta_2(1-\theta_1)t^{\theta_2-1}}{\Lambda(\theta_1)}\Xi_4\left(t, \tilde{\mathrm{I}}\right) + \frac{\theta_2\theta_1}{\Lambda(\theta_1)\Gamma(\theta_1)} \int_0^t s^{\theta_2-1}(t-s)^{\theta_1-1}\Xi_4\left(s, \tilde{\mathrm{I}}\right) ds. \tag{26}$$

Now,

$$\begin{aligned}
\left\|\mathrm{S_t}-\tilde{\mathrm{S}}_\mathrm{t}\right\| &= \left\|\frac{\theta_2\left(1-\theta_1\right)t^{\theta_2-1}}{\Lambda(\theta_1)}\right.\\
&\left(\Xi_1\left(t,\mathrm{S}_t\right)-\Xi_1\left(t,\tilde{\mathrm{S}}_t\right)\right)\\
&+\frac{\theta_2\theta_1}{\Lambda(\theta_1)\Gamma\left(\theta_1\right)}\int_0^t s^{\theta_2-1}\left(t-s\right)^{\theta_1-1}\\
&\left.\left(\Xi_1\left(t,\mathrm{S}_t\right)-\Xi_1\left(t,\tilde{\mathrm{S}}_t\right)\right)ds\right\|,\\
&\leq \frac{\theta_2\left(1-\theta_1\right)t^{\theta_2-1}}{\Lambda(\theta_1)}\left\|\Xi_1\left(t,\mathrm{S}_t\right)-\Xi_1\left(t,\tilde{\mathrm{S}}_t\right)\right\|\\
&+\frac{\theta_1\theta_2}{\Lambda(\theta_1)\Gamma\left(\theta_1\right)}\int_0^t s^{\theta_1-1}\left(t-s\right)^{\theta_1-1}\\
&\left\|\Xi_1\left(t,\mathrm{S}_t\right)-\Xi_1\left(t,\tilde{\mathrm{S}}_t\right)\right\|ds,\\
&\leq \frac{\theta\left(1-\vartheta\right)\mathrm{t}^{\theta-1}}{\Lambda(\vartheta)}L_1\left\|\mathrm{S_t}-\tilde{\mathrm{S}}_\mathrm{t}\right\|+\frac{\vartheta\theta}{\Lambda(\vartheta)\Gamma\left(\vartheta\right)}\\
&\int_0^{\mathrm{t}} s^{\theta-1}\left(\mathrm{t}-s\right)^{\vartheta-1}L_1\left\|\mathrm{S_t}-\tilde{\mathrm{S}}_\mathrm{t}\right\|ds,\\
&\leq \left(\frac{\theta_2\left(1-\theta_1\right)t^{\theta-1}}{\Lambda\left(\theta_1\right)}+\frac{\theta_1\theta_2}{\Lambda\left(\theta_1\right)\Gamma\left(\theta_1\right)}\right.\\
&\left.\int_0^t s^{\theta_2-1}\left(t-s\right)^{\theta_1-1}ds\right)L_1\left\|\mathrm{S}_t-\tilde{\mathrm{S}}_t\right\|,\\
&\leq \left(\frac{\theta_1\left(1-\theta_2\right)t^{\theta_2-1}}{\Lambda\left(\theta_1\right)}+\frac{\theta_1\Gamma\left(\theta_2+1\right)t^{\theta_1+\theta_2-1}}{\Lambda\left(\theta_1\right)\Gamma\left(\theta_1+\theta_2+1\right)}\right)\\
&L_1\left\|\mathrm{S}_t-\tilde{\mathrm{S}}_t\right\|, \qquad (27)
\end{aligned}$$

This implies that

$$\begin{aligned}
&\left(1-\left(\frac{\theta_1\left(1-\theta_2\right)t^{\theta_2-1}}{\Lambda\left(\theta_1\right)}+\frac{\theta_1\Gamma\left(\theta_2+1\right)t^{\theta_1+\theta_2-1}}{\Lambda\left(\theta_1\right)\Gamma\left(\theta_1+\theta_2+1\right)}\right)L_1\right)\\
&\left\|\mathrm{S}_t-\tilde{\mathrm{S}}_t\right\|\leq 0, \qquad (28)
\end{aligned}$$

Therefore, $\left\|\mathrm{S}_t-\tilde{\mathrm{S}}_t\right\|=0$. Hence, $\mathrm{S}_t=\tilde{\mathrm{S}}_t$. In a similar way, we can prove$\mathrm{I}_t=\tilde{\mathrm{I}}_t$, $\mathrm{Q}_t=\tilde{\mathrm{Q}}_t$, $\mathrm{I}=\tilde{\mathrm{I}}$.

Hence, the epidemic model-based DDoS attack with FFAB has a unique solution.

4. Ulam–Hyers stability

In this section, we establish the UH stability of **Equation** (6). To proceed, we first present the necessary definition.

Definition 4.1. Equation (6) has UH stability if there exist constants $\xi_i>0$, $i=1,2,3,4$,satisfying the following condition:

For every $\Xi_i>0$, $i=1,2,3,4$, if:

$$\begin{cases}
\left|{}_0^{FFAB}D_t^{\theta_1,\theta_2}\mathrm{S_t}-\Xi_1\left(t,\mathrm{S}_t\right)\right|\leq\xi_1,\\
\left|{}_0^{FFAB}D_t^{\theta_1,\theta_2}\mathrm{I_t}-\Xi_2\left(t,\mathrm{I}_t\right)\right|\leq\xi_2,\\
\left|{}_0^{FFAB}D_t^{\theta_1,\theta_2}\mathrm{Q_t}-\Xi_3\left(t,\mathrm{Q}_t\right)\right|\leq\xi_3,\\
\left|{}_0^{FFAB}D_t^{\theta_1,\theta_2}\mathrm{I}-\Xi_4\left(t,\mathrm{I}\right)\right|\leq\xi_4.
\end{cases} \qquad (29)$$

there exists a solution $\tilde{\mathrm{S}}_t$,$\tilde{\mathrm{I}}_t$, $\tilde{\mathrm{Q}}_t$, $\tilde{\mathrm{I}}$,of **Equation** (6) that satisfies the given model, such that

$$\begin{cases}
\left\|\mathrm{S}_t-\tilde{\mathrm{S}}_t\right\|\leq\eta_1\xi_1, \left\|\mathrm{I}_t-\tilde{\mathrm{I}}_t\right\|\leq\eta_2\xi_2,\\
\left\|\mathrm{Q}_t-\tilde{\mathrm{Q}}_t\right\|\leq\eta_3\xi_3, \left\|\mathrm{I}-\tilde{\mathrm{I}}\right\|\leq\eta_4\xi_4.
\end{cases} \qquad (30)$$

Remark 1. Suppose that S_t represents a solution of the first inequality in **Equation** (29). This holds if there exists a continuous function $\mathrm{h_i}$ such that

(i) $\left|\mathrm{h}_1\left(t\right)\right|<\xi_1$
(ii) ${}_0^{FFAB}D_t^{\theta_1,\theta_2}\mathrm{S}_t=\Xi_1\left(t,\mathrm{S}_t\right)+\mathrm{h}_1\left(t\right).$

In a similar manner, corresponding functions $\mathrm{h_i}$ for $i=2,3,4$ can be introduced for the remaining classes of **Equation** (29).

Theorem 4.1. Assume that hypothesis H holds. Then, **Equation** (6) is UH stable if

$$\begin{aligned}
&\left(\frac{\theta_2\left(1-\theta_1\right)t^{\theta_2-1}}{\Lambda\left(\theta_1\right)}+\frac{\theta_1\Gamma\left(\theta_2+1\right)\mathrm{t}^{\theta_1+\theta_2-1}}{\Lambda\left(\theta_1\right)\Gamma\left(\theta_1+\theta_2+1\right)}\right)\\
&L_i\leq 1 \text{ for } i=1,2,3,4. \qquad (31)
\end{aligned}$$

Proof. Let $\xi_1>0$ and $\mathrm{S_t}$ be arbitrary functions such that

$$\left\|{}_0^{FFAB}D_t^{\theta_1,\theta_2}\mathrm{S}_t-\Xi_1\left(t,\mathrm{S}_t\right)\right\|\leq\xi_1. \qquad (32)$$

According to **Remark 1**, there exists a function $\mathrm{h_1}$such that $\left\|\mathrm{h}_1\left(t\right)\right\|<\xi_1$and it fulfils the condition that

$${}_0^{FFAB}D_t^{\theta_1,\theta_2}\mathrm{S}_t=\Xi_1\left(t,\mathrm{S}_t\right)+\mathrm{h}_1\left(t\right). \qquad (33)$$

Accordingly, we get

$$\begin{aligned}
\mathrm{S}_t &= \mathrm{S}_t\left(0\right)+\frac{\theta_2\left(1-\theta_1\right)t^{\theta_2-1}}{\Lambda(\theta_1)}\Xi_1\left(t,\mathrm{S}_t\right)\\
&+\frac{\theta_1\theta_2}{\Lambda(\theta_1)\Gamma\left(\theta_1\right)}\int_0^t s^{\theta_2-1}\left(t-s\right)^{\theta_1-1}\Xi_1\left(s,\mathrm{S}_t\right)ds\\
&+\frac{\theta_2\left(1-\theta_1\right)t^{\theta_2-1}}{\Lambda(\theta_1)}\mathrm{h}_1\left(t\right)+\frac{\theta_1\theta_2}{\Lambda(\theta_1)\Gamma\left(\theta_1\right)}\\
&\int_0^t s^{\theta_2-1}\left(t-s\right)^{\theta_1-1}\mathrm{h}_1\left(s\right)ds. \qquad (34)
\end{aligned}$$

Let $\tilde{\mathrm{S}}_{\mathrm{t}}$ be the unique solution of **Equation** (6). Then

$$\tilde{\mathrm{S}}_{\mathrm{t}}(\mathrm{t}) = \tilde{\mathrm{S}}_{\mathrm{t}}(0) + \frac{\theta_2(1-\theta_1)t^{\theta_2-1}}{\Lambda(\theta_1)}\Xi_1\left(t,\tilde{\mathrm{S}}_t\right) + \frac{\theta_1\theta_2}{\Lambda(\theta_1)\Gamma(\theta_1)}\int_0^t s^{\theta_2-1}(t-s)^{\theta_1-1}\Xi_1\left(s,\tilde{\mathrm{S}}_t\right)ds. \tag{35}$$

Hence,

$$\begin{aligned}
&\|\mathrm{S}_t-\tilde{\mathrm{S}}_t\| \le \frac{\theta_2(1-\theta_1)t^{\theta_2-1}}{\Lambda(\theta_1)}\\
&\left\|\Xi_1(t,\mathrm{S}_t)-\Xi_1\left(t,\tilde{\mathrm{S}}_t\right)\right\|\\
&+\frac{\theta_1\theta_2}{\Lambda(\theta_1)\Gamma(\theta_1)}\int_0^t s^{\theta_2-1}(t-s)^{\theta_1-1}\\
&\left\|\Xi_1(t,\mathrm{S}_t)-\Xi_1\left(t,\tilde{\mathrm{S}}_t\right)\right\|ds\\
&+\frac{\theta_2(1-\theta_1)t^{\theta_2-1}}{\Lambda(\theta_1)}\|\mathrm{h}_1(t)\|+\frac{\theta_1\theta_2}{\Lambda(\theta_1)\Gamma(\theta_1)}\\
&\int_0^{\mathrm{t}} s^{\theta_2-1}(t-s)^{\theta_1-1}\|\mathrm{h}_1(t)\|ds,\\
&\le\left(\frac{\theta_2(1-\theta_1)t^{\theta_2-1}}{\Lambda(\theta_1)}+\frac{\theta_1\Gamma(\theta_2+1)t^{\theta_1+\theta_2-1}}{\Lambda(\theta_1)\Gamma(\theta_1+\theta_2+1)}\right)\\
&\quad L_1\|\mathrm{S}_t-\tilde{\mathrm{S}}_t\|\\
&+\left(\frac{\theta_2(1-\theta_1)t^{\theta_2-1}}{\Lambda(\theta_1)}+\frac{\theta_1\Gamma(\theta+1)t^{\theta_1+\theta_2-1}}{\Lambda(\theta_1)\Gamma(\theta_1+\theta_2+1)}\right)\xi_1,\\
&\|\mathrm{S}_t-\tilde{\mathrm{S}}_t\| \le \frac{\left(\frac{\theta_2(1-\theta_1)t^{\theta_2-1}}{\Lambda(\theta_1)}+\frac{\theta_1\Gamma(\theta_2+1)t^{\theta_1+\theta_2-1}}{\Lambda(\theta_1)\Gamma(\theta_1+\theta_2+1)}\right)\xi_1}{1-\left(\frac{\theta_2(1-\theta_1)t^{\theta_2-1}}{\Lambda(\theta_1)}+\frac{\theta_1\Gamma(\theta_2+1)t^{\theta_1+\theta_2-1}}{\Lambda(\theta_1)\Gamma(\theta_1+\theta_2+1)}\right)L_1}.
\end{aligned} \tag{36}$$

Then,

$$\left\|\mathrm{S}_{\mathrm{t}}-\tilde{\mathrm{S}}_{\mathrm{t}}\right\| \le \xi_1\eta_1 \tag{37}$$

where $\eta_1 = \frac{\left(\frac{\theta_2(1-\theta_1)t^{\theta_2-1}}{\Lambda(\theta_1)}+\frac{\theta_1\Gamma(\theta_2+1)t^{\theta_1+\theta_2-1}}{\Lambda(\theta_1)\Gamma(\theta_1+\theta_2+1)}\right)}{1-\left(\frac{\theta_2(1-\theta_1)t^{\theta_2-1}}{\Lambda(\theta_1)}+\frac{\theta_1\Gamma(\theta_2+1)t^{\theta_1+\theta_2-1}}{\Lambda(\theta_1)\Gamma(\theta_1+\theta_2+1)}\right)L_1}$.

Similarly, we have

$$\left\|\mathrm{I}_t-\tilde{\mathrm{I}}_t\right\| \le \eta_2\xi_2, \left\|\mathrm{Q}_t-\tilde{\mathrm{Q}}_t\right\| \le \eta_3\xi_3, \left\|\mathrm{I}-\tilde{\mathrm{I}}\right\| \le \eta_4\xi_4. \tag{38}$$

Hence, **Equation** (6) is UH stable.

5. Basic reproduction number $\mathbf{R}_0$

The basic reproduction number describes the average number of new infections generated by a single infectious node over its entire infectious period, assuming it interacts only with susceptible nodes.[38] This quantity is a key indicator in both biological epidemic modeling and cyber-attack analysis, as it helps determine whether an infection or attack will spread or die out. The reproduction number for each population can be evaluated separately according to its specific transmission dynamics.

From **Equations** (3) and (4), the infectious compartments are $\mathrm{I_t}$and I_a the targeted and attacking populations, respectively. Thus, the infected state vector is:

$$\mathrm{X}=(\mathrm{I_t},\mathrm{I}_a)^T. \tag{39}$$

The infection dynamics for the targeted population are governed by:

$$\frac{d\mathrm{I}_t}{dt}=\beta\mathrm{S}_t\mathrm{I}-\gamma\mathrm{I}_t, \tag{40}$$

The rate of new infections entering $\mathrm{I}_t$is

$$F_t=\beta\mathrm{S}_t\mathrm{I}. \tag{41}$$

The rate of removal from $\mathrm{I}_t$due to recovery or quarantine is

$$V_t=\gamma\mathrm{I}_t \tag{42}$$

At the disease-free equilibrium (DFE)

$$\mathrm{S}_t=1,\ \mathrm{I}_a=0. \tag{43}$$

Evaluating the partial derivative of F_t with respect to $\mathrm{I}_a$at the DFE gives

$$\left.\frac{\partial F_t}{\partial \mathrm{I}_t}\right|_{\mathrm{DEF}}=\beta. \tag{44}$$

Similarly,

$$\left.\frac{\partial V_t}{\partial \mathrm{I}_t}\right|_{\mathrm{DEF}}=\gamma. \tag{45}$$

Thus, the basic reproduction number for the targeted population is

$$R_{0t}=\frac{\beta}{\gamma}. \tag{46}$$

This quantity represents the average number of newly infected targeted nodes generated by a single infectious attacker during its infectious period.

The infection dynamics for the attacking population are given by

$$\frac{d\mathrm{I}_a}{dt}=\beta\mathrm{S}_a\mathrm{I}_a-(\mu+\varepsilon)\mathrm{I}_a. \tag{47}$$

The rate of new infections is

$$F_a=\beta\mathrm{S}_a\mathrm{I}_a. \tag{48}$$

The rate of removal due to natural death and defense mechanisms is

$$V_a=(\mu+\varepsilon)\mathrm{I}_a. \tag{49}$$

At the DFE,

$$\mathrm{S}_a=1. \tag{50}$$

Evaluating the derivatives at the DFE yields

$$\left.\frac{\partial F_a}{\partial \mathrm{I}_a}\right|_{\mathrm{DEF}}=\beta,\quad \left.\frac{\partial V_a}{\partial \mathrm{I}_a}\right|_{\mathrm{DEF}}=\mu+\varepsilon. \tag{51}$$

Hence, the reproduction number for the attacking population is

$$R_{0a} = \frac{\beta}{\mu + \varepsilon}. \tag{52}$$

By combining these, we found a single reproduction number in the host vector model of epidemiology as $R_0 = \sqrt{\frac{\beta^2}{(\mu+\varepsilon)\gamma}}$.

6. Stability analysis

In this section, we examined the stability of the system from two perspectives: local stability and global stability.

Theorem 5.1. Within the positively invariant regionΩ, the system described in **Equation** (5) admits two equilibrium points. The first is the DFE $\mathrm{E}_0 = (\mathrm{S_t}, \mathrm{I_t}, \mathrm{Q_t}, \mathrm{I}) = (1,0,0,0)$,and the second is the unique endemic equilibrium $\mathrm{E}^* = (\mathrm{S_t^*}, \mathrm{I_t^*}, \mathrm{Q_t^*}, \mathrm{I}^*)$, which exists whenever the inequality $\beta > (\mu + \varepsilon)$ holds.

Proof. For the complete proof, see Rao et al.[38]

Theorem 5.2. For **Equation** (5), the DFE E_0 is locally asymptotically stable within the regionΩwhenever $R_{0a} < 1$. Conversely, if $R_{0a} > 1$, this equilibrium becomes unstable.

Proof. For the complete proof, see Rao et al.[38]

7. Sensitivity analysis of the basic reproduction number ($\mathbf{R}_0$)

Sensitivity analysis is performed to quantify how variations in model parameters influence the magnitude of R_0. Understanding the relative importance of each parameter helps identify which control strategies are most effective in reducing the spread of attacking nodes. The ratio of the relative change in the variable to the relative change in the parameter is known as the normalized forward sensitivity index of a variable with respect to a parameter. Partial derivatives are used to define the sensitivity index if the variable is a differentiable function of the parameter.38

Definition 7.1. The normalized forward sensitivity index of a variable ϕ that depends differentiably on a parameter is defined as:

$$\Upsilon_z^{\phi} = \frac{\partial \phi}{\partial z}\frac{z}{\phi} \tag{53}$$

Table 2 provides the parameter sensitivity indices.

The sensitivity results reveal that β is the most influential parameter, exhibiting a normalized index of +1. This shows that the propagation capability of attacking nodes is the primary driver of network compromise. Any increase in β proportionally raisesR_0, making the attack substantially more severe. The recovery rate γ decreases R_0 with a constant elasticity of -0.5, demonstrating that strengthening node recovery mechanisms effectively mitigates attack sustainability. Between the defensive parameters, the neutralization rate εhas a stronger suppressive effect than the natural removal rateμ. This indicates that system-level defense mechanisms are more impactful in reducing attack reproduction compared to the natural decay of attacking nodes. Overall, the results indicate that reducing the attack transmission rate and enhancing targeted node recovery are the most impactful strategies for destabilizing the attacking population and ensuring the network remains resilient against DDoS activity.

Table 2. Parameter sensitive indices

Parameter	Value used	Sensitivity index
β	0.4	1.0000
γ	0.35	−0.5000
μ	0.15	−0.1667
ε	0.3	−0.3333

8. Results and discussion

To support the theoretical findings, numerical simulations are provided in this section. The Adams–Bashforth method was used to solve the FF DDoS model given in **Equation** (6). To reflect realistic DDoS attack behavior in a CIs environment, two scenarios were considered, each consisting of two cases. These cases were considered by varying the infection transmission rate β and the quarantine rate of infected attacking nodes γ, as summarized in **Table 3**. The parameter values were taken from existing studies to guarantee practical relevance.[38]

Example 1. The numerical results for an unsuccessful DDoS attack are presented in **Figure 3**. The system was initialized using the ICs $\mathrm{S}_t(0) = 0.7$, $\mathrm{I}_t(0) = 0.2, \mathrm{Q}_t(0) = 0.1$, and $\mathrm{I}(0) = 0.5$,together with the parameter settings $\beta = 0.4$, $\gamma = 0.35, \eta = 0.4$, $\varepsilon = 0.3$, $\varepsilon_t = 0.3$, and $\mu = 0.15$,reported in Rao et al.[38] Under this configuration, the basic reproduction number for the attacking population is found to be$R_{0a} < 1$, indicating that the attack cannot sustain itself within the network. **Figure 4** depicts how varying the FF orders $\theta_1 = \theta_2$ influences the time evolution of all compartments. Four distinct FF orders were examined $\theta_1 = \theta_2 = 1, 0.95, 0.9,$ and 0.85—to understand how memory and fractal effects modify the system's dynamics.

Table 3. Scenarios and cases for the distributed denial-of-service model

Scenario	Case	.5		Parameter		
		β	Γ	η	ε	ε_t
1	1	0.40	0.35	0.40	0.30	0.30
	2	0.70	0.35	0.40	0.30	0.30
2	1	0.20	0.20	0.40	0.30	0.30
	2	0.20	0.10	0.40	0.30	0.30

In **Figure 4A**, the susceptible S_t shows that lower FF orders lead to a slower recovery toward equilibrium. When $\theta_1 = \theta_2 = 1$, the curve follows the classical behavior, reaching stability faster. However, as the FF order $\theta_1 = \theta_2 = 0.95, 0.9,$ and 0.85decreases, the trajectory becomes more gradual, reflecting a stronger memory effect in the system and delaying the stabilization of the susceptible population. **Figure 4B** depicts the infected classI_t, where a similar trend is observed. For integer order, the infection decays quickly, whereas for FF orders $\theta_1 = \theta_2 = 0.95, 0.9,$ and 0.85,the decay is noticeably slower. This shows that lower orders preserve more historical influence, causing the infection to persist longer before dying out.

In **Figure 4C**, the quarantined population$Q_t$initially increases and then declines. At $\theta_1 = \theta_2 = 1$, the decline occurs sharply, but for smaller orders, the decay is smoother and more stretched over time. This again highlights the impact of fractional dynamics in extending the influence of earlier states, which can better capture delayed responses in real-world systems. Finally, **Figure 4D** displays the attacking classI. All curves show a decreasing trend, but the rate of decay is highly dependent on the order. The classical case approaches zero rapidly, while the FF case exhibits a prolonged tail, indicating slower attenuation of the attack intensity.

Scenario 1. Figure 5 depicts Case 1, where two attack cases were analyzed under different infection transmission rates and FF orders. Case 1 shows a moderate DDoS attack with$\beta = 0.4$, while case 2 represents a more aggressive attack scenario with$\beta = 0.7$. For each case, the system dynamics were examined under different FF orders. The graphical results indicate that increasing the FF memory effect slows the decay process and delays the stabilization of the infected and quarantined populations, indicating persistent attack influence and delayed mitigation. In comparison with Case 1, Case 2 shows more rapid propagation and higher attack intensity across all state variables, reflecting the impact of a higher transmission rate. This shows that the FF model effectively captures both varying attack strengths and memory-dependent dynamics in realistic DDoS scenarios.

Scenario 2. Figure 6 depicts the impact of two cases under different quarantine rates of infected attacking nodes and infection transmission rates γ and β for various FF orders. In Case 1, the infected and active attacking populations decay rapidly to low levels due to stronger quarantine and reduced transmission, and this decay is faster for lower fractional orders, showing that memory effects enhance mitigation. In contrast, Case 2 exhibits higher steady-state levels of infected nodes, indicating weaker control despite initial transients. Across all subfigures, decreasing the FF order from $\theta_1 = \theta_2 = 1, 0.95,$ and 0.9 smooths the dynamics and accelerates convergence to equilibrium, indicating that the FF order strongly affects both the spread and containment dynamics. Overall, Case 1 is more effective than Case 2, and lower FF orders provide better suppression of infection and attack propagation in **Scenario 2**.

Example 2. The numerical results for the unsuccessful attack are presented in **Figure 7**. The system is initialized with $S_t(0) = 0.7$, $I_t(0) = 0.2, Q_t(0) = 0.1,$ and $I(0) = 0.5$,together with the parameter settings $\beta = 0.7, \gamma = 0.35, \eta = 0.4, \varepsilon = 0.3, \varepsilon_t = 0.3,$ and $\mu = 0.15,$ adopted from Rao et al.[38] For this configuration, the basic reproduction number for the attacking population is obtained as $R_{0a} = 1.556$.[38] Since$R_{0a} > 1$, **Figure 7** confirms that the system approaches an endemic equilibrium, indicating its stability.

Figures 8 and 9 show the phase-plane dynamics between infectious targeted nodes I_t and quarantine targeted nodes $Q_t$for different FF orders. In **Figure 8**, since $R_{0a} < 1$, all trajectories move toward the disease-free state, showing that the infection eventually dies out. Although lower FF orders result in slower convergence due to stronger memory effects, the system remains stable and approaches the origin.

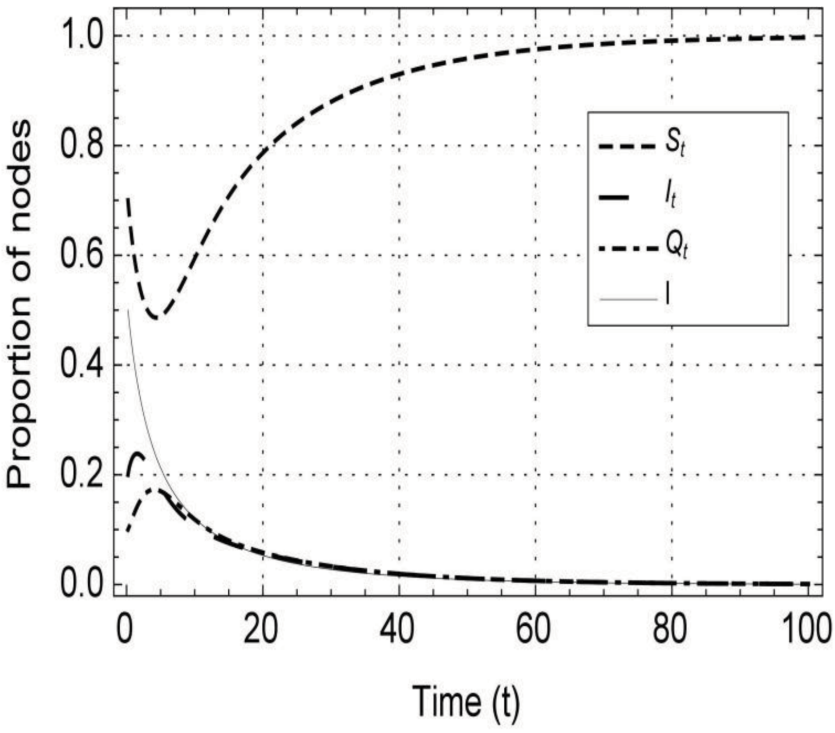

Figure 3. Local stability of the disease-free equilibrium of the model

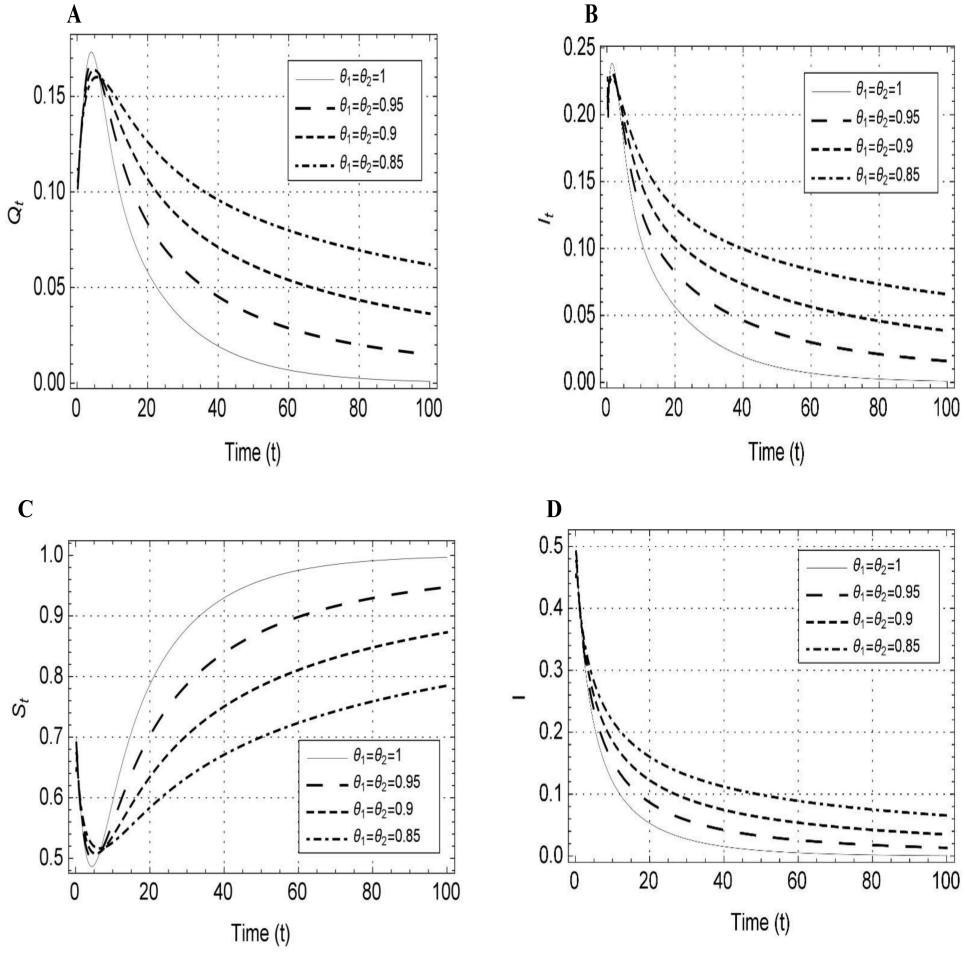

Figure 4. Local stability of the disease-free equilibrium for different fractal–fractional orders: (A) S_t, (B) I_t, (C) Q_t, and (D) I

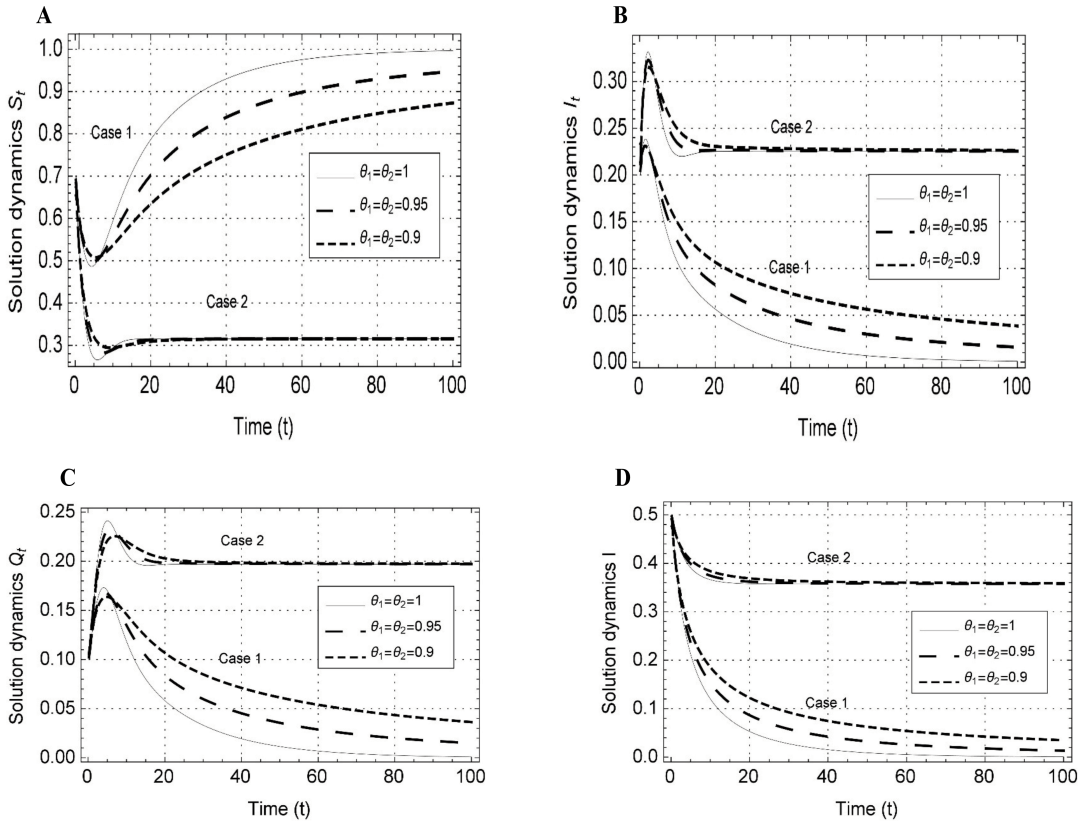

Figure 5. Dynamics of the distributed denial-of-service model for Scenario 1, showing the effect of different infection transmission ratesβ on the system behavior: (A) S_t, (B) I_t, (C) Q_t, and (D) I

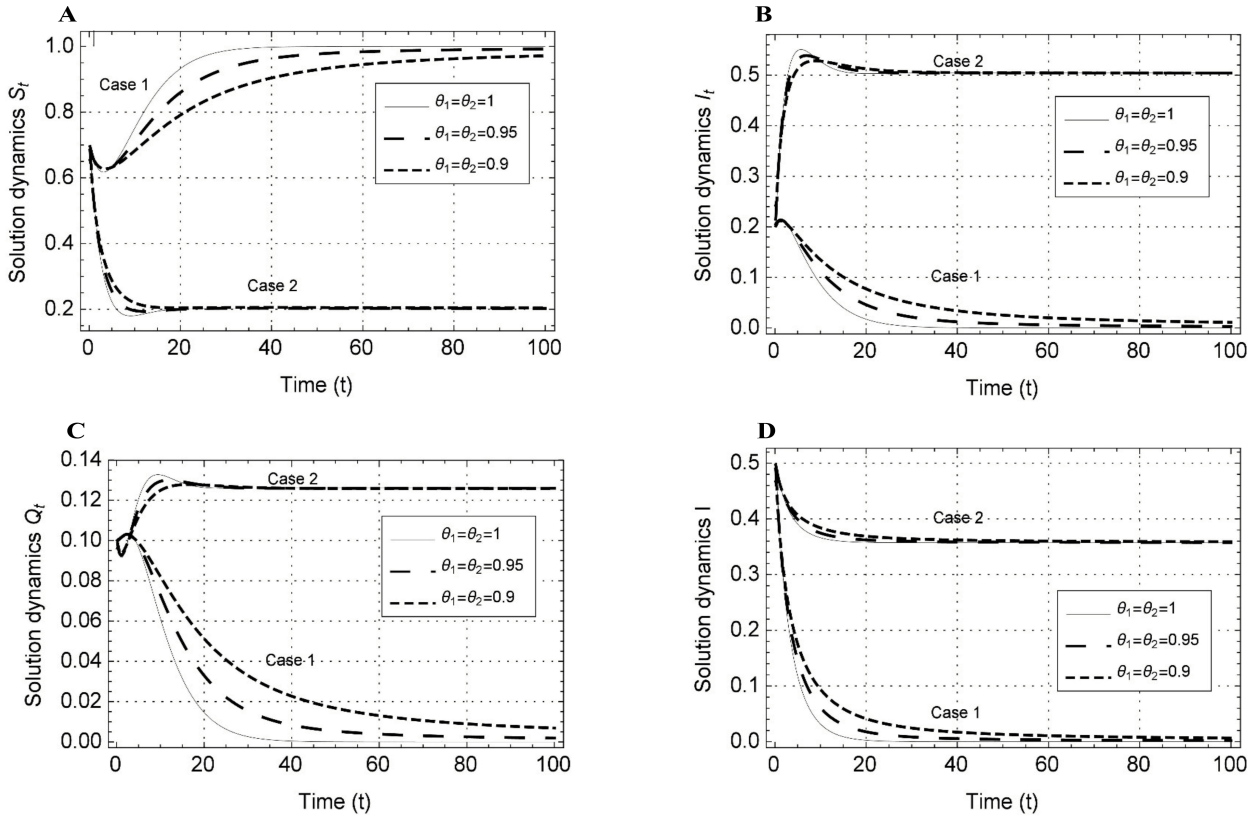

Figure 6. Dynamics of the model variable for Scenario 2 under Case 1 and Case 2, showing the effects of different quarantine rates and infection transmission rates β and γ for varying fractal–fractional orders: (A) S_t, (B) I_t, (C) Q_t, and (D) I

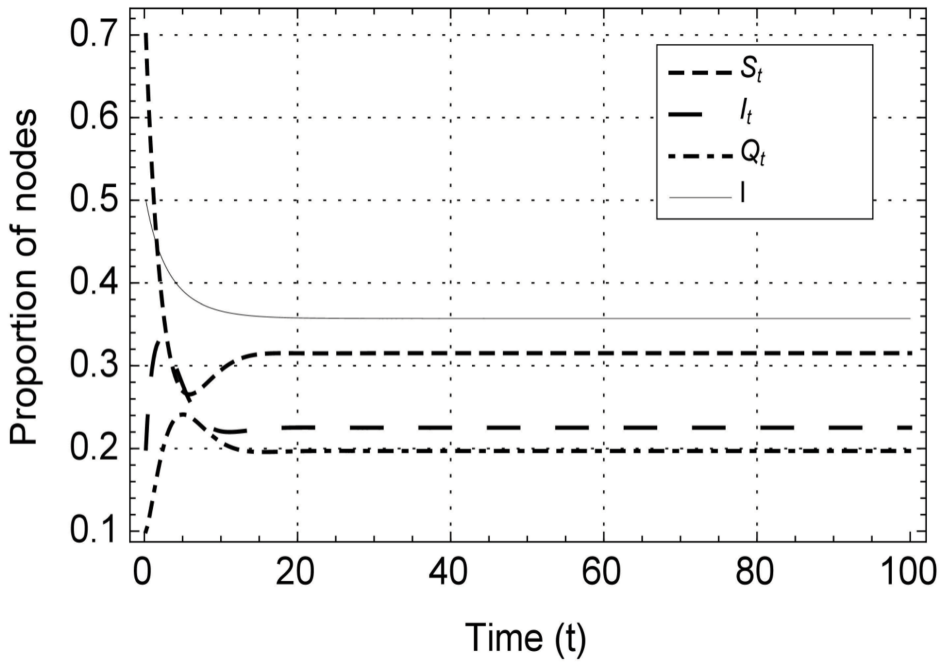

Figure 7. Local stability of the endemic equilibrium of the model

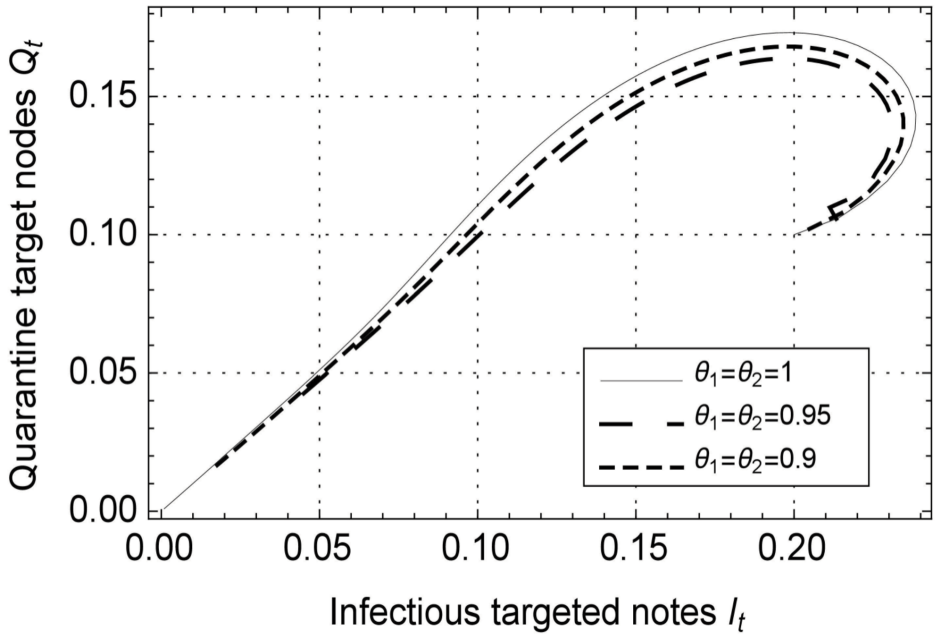

Figure 8. Phase-plane dynamics of infectious targeted nodes versus quarantine targeted nodes when $R_{0a} < 1$ for different fractal–fractional orders

In contrast, in **Figure 9**, since $R_{0a} > 1$, the trajectories form closed loops, indicating the presence of an endemic equilibrium. The loops widen for smaller FF orders, reflecting prolonged oscillations between infectious and quarantined nodes. This behavior highlights how memory effects intensify and extend the persistence of infection when $R_{0a} > 1$.

The substantive novelty of the proposed FFAB-based DDoS model lies in its ability to simultaneously capture network heterogeneity and long-term memory effects, which are not adequately represented in existing integer order or standard fractional order DDoS models. Real-world network infrastructures are characterized by irregular topologies, non-uniform traffic flows, and delayed mitigation responses caused by filtering latency, routing congestion, and adaptive defense mechanisms. While classical models assume uniform interactions and instantaneous response, and

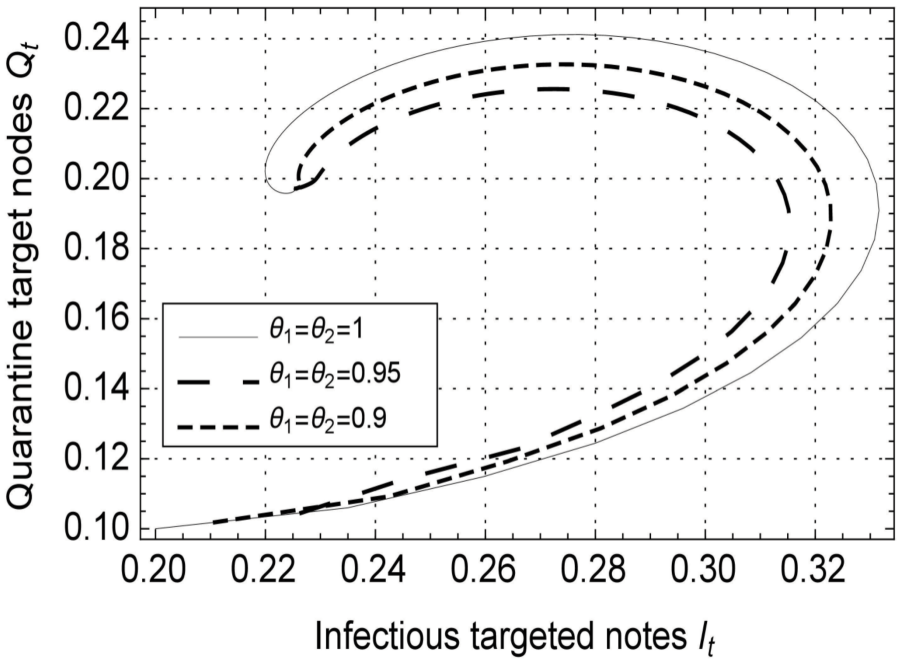

Figure 9. Phase-plane dynamics of infectious targeted nodes versus quarantine targeted nodes when $R_{0a} > 1$ for different fractal–fractional orders

fractional order models account only for temporal memory, the proposed FF formulation incorporates both spatial irregularity and persistent attack influence. This enhanced modeling capability provides actionable engineering insights for cybersecurity defense, including optimized tuning of mitigation parameters, improved timing of intervention strategies, and more effective allocation of defensive resources in large-scale and heterogeneous networks.

9. Conclusion

We developed an FF formulation of the DDoS epidemic model to better capture the memory and irregular behavior present in real network traffic. By incorporating the FFAB derivative, the model is able to reflect both long-term dependence and structural complexity, offering a more flexible representation compared to classical integer-order systems. Within this framework, the existence and uniqueness of solutions were established, and UH stability was examined to ensure the reliability of the model. The threshold conditions under which an attack either dies out or persists in the network were identified by the stability analysis at the endemic and infection-free equilibria. These findings are further demonstrated by numerical tests conducted using the Adams–Bashforth method for various combinations of FF orders. The simulations demonstrated that lower FF orders introduce stronger memory effects, slowing the decay of infection and extending the influence of past states.

Overall, the results demonstrate the utility of FF operators for simulating the dynamics of cyber-attacks. The FFAB formulation captures behaviors that classical models tend to overlook, such as delayed response, prolonged infection persistence, and more realistic quarantine effects. These insights may assist in designing stronger defense strategies and improving the resilience of modern CI networks against coordinated DDoS attacks. For future studies, the proposed DDoS attack model may be coupled with network anomaly detection and monitoring mechanisms to enable timely identification of attack onset and parameter variations, thereby enhancing its applicability in data-driven network security and defense planning frameworks.

Acknowledgments

None.

Funding

This study was funded by the fellowship scheme received from Universiti Teknikal Malaysia Melaka.

Conflict of interest

The authors declare that they have no known competing financial interests or personal relationships that could have appeared to influence the work reported in this paper.

Author contributions

Conceptualization: Mumtaz Ali, Nooraini Zainuddin, Nazreen Waeleh
Formal analysis: Mumtaz Ali, Nazreen Waeleh, Hanita Daud
Methodology: Mumtaz Ali
Software: Mumtaz Ali, Rahimah Jusoh
Writing–original draft: Mumtaz Ali, Nooraini Zainuddin
Writing–review & editing: Nooraini Zainuddin, Rahimah Jusoh, Hanita Daud

Availability of data

Not applicable.

AI tools statement

All authors confirm that no AI tools were used in the preparation of this manuscript.

References

1. George AS, Baskar T, Srikaanth PB. Cyber threats to critical infrastructure: assessing vulnerabilities across key sectors. *PUIIJ.* 2024;2(1):51–75. https://www.doi.org/10.5281/zenodo.10639463
2. Ten C-W, Manimaran G, Liu C-C. Cybersecurity for critical infrastructures: attack and defense modeling. *IEEE Trans Syst Man Cybern A Syst Hum.* 2010;40(4):853–865. https://www.doi.org/10.1109/TSMCA.2010.2048028
3. Yu A, Kolotylo I, Hashim HA, Eltoukhy AEE. Electronic warfare cyberattacks, countermeasures and modern defensive strategies of UAV avionics: a survey. *IEEE Access.* 2025;13:68660–68681. https://www.doi.org/10.1109/ACCESS.2025.3561068
4. Ahmad I, Bakar AA, Jan R, Yussof S. Dynamic behaviors of a modified computer virus model: insights into parameters and network attributes. *Alex Eng J.* 2024;103:266–277. https://www.doi.org/10.1016/j.aej.2024.06.009
5. Osanaiye O, Choo K-KR, Dlodlo M. Distributed denial of service (DDoS) resilience in cloud: review and conceptual cloud DDoS mitigation framework. *J Netw Comput Appl.* 2016;67:147–165. https://www.doi.org/10.1016/j.jnca.2016.01.001
6. Nour B, Mastorakis S, Ullah R, Stergiou N. Information-centric networking in wireless environments: security risks and challenges. *IEEE Wirel Commun.* 2021;28(2):121–127. https://www.doi.org/10.1109/MWC.001.2000245
7. Jayadatta S. Impact and effect of spyware, adware, and malware on digital environment in modern society. In: *Digital Transformation in the Customer Experience.* Apple Academic Press; 2025:73-89. https://www.doi.org/10.1201/9781003560449
8. Goni A, Jahangir MUF, Chowdhury RR. A study on cyber security: analyzing current threats, navigating complexities, and implementing prevention strategies. *Int J Res Sci Innov.* 2024;10(12):507–522. https://www.doi.org/10.51244/IJRSI.2023.1012039
9. Mohanty S, Parida C, Mahanta G, Nayak PK. A sensitivity analysis approach to investigating virus transmission in interconnected computer network. *IAENG Int J Comput Sci.* 2025;52(9):3459–3466.
10. Hnamte V, Najar AA, Nhung-Nguyen H, Hussain J, Sugali MN. DDoS attack detection and mitigation using deep neural network in SDN environment. *Comput Secur.* 2024;138:103661. https://www.doi.org/10.1016/j.cose.2023.103661
11. Casado-Vara R, Severt M, Díaz-Longueira A, Rey ÁMd, Calvo-Rolle JL. Dynamic malware mitigation strategies for iot networks: a mathematical epidemiology approach. *Mathematics.* 2024;12(2):250. https://www.doi.org/10.3390/math12020250
12. Barbero G, Evangelista LR, Zola RS, Lenzi EK, Scarfone AM. A brief review of fractional calculus as a tool for applications in physics: adsorption phenomena and electrical impedance in complex fluids. *Fractal Fract.* 2024;8(7):369. https://www.doi.org/10.3390/fractalfract8070369
13. Xue D, Bai L. Introduction to fractional calculus. In: *Fractional Calculus: High-precision Algorithms and Numerical Implementations.* Springer; 2024:1–17. https://www.doi.org/10.1007/978-981-99-2070-9_1
14. Rokaya M, Hemdan DI, Alzain MA, Atlam E-S. A novel fractional-order model with data-driven validation for the dynamics of complex epidemic spreading in networks. *Int J Optim Control Theor Appl.* 2025;16(1):111–137. https://www.doi.org/10.36922/IJOCTA025220107
15. Ali M, Khan NA, Ayaz M, Khan NA. Existence and uniqueness analysis of a fractional atmospheric system using Haar-based operational matrices. *Int J Optim Control Theor Appl.* 2025;16(1):91–110. https://www.doi.org/10.36922/IJOCTA025320140
16. Dilmi M, Benallia M. A new general conformable fractional derivative and some applications. *J Fract Calc Appl.* 2025;16(2):1–16. https://www.doi.org/10.21608/jfca.2025.402920.1179

17. Abdelouahab M-S, Hamri N-E. The Grünwald–Letnikov fractional-order derivative with fixed memory length. *Mediterr J Math.* 2016;13(2):557–572. https://www.doi.org/10.1007/s00009-015-0525-3
18. Caputo M, Fabrizio M. A new definition of fractional derivative without singular kernel. *Prog Fract Differ Appl.* 2015;1(2):73–85. https://www.doi.org/10.12785/pfda/010201
19. Almeida R. A Caputo fractional derivative of a function with respect to another function. *Commun Nonlinear Sci Numer Simul.* 2017;44:460–481. https://www.doi.org/10.1016/j.cnsns.2016.09.006
20. Jarad F, Abdeljawad T, Baleanu D. Caputo-type modification of the Hadamard fractional derivatives. *Adv Differ Equ.* 2012;2012(1):142. https://www.doi.org/10.1186/1687-1847-2012-142
21. Thangamani S, Baleanu D, Lourdu P, Yousif MA, Mohammed PO. New horizons in analytic function classes induced by the Erdélyi–Kober fractional integral operators. *Int J Optim Control Theor Appl.* 2025;16(1):176–190. https://www.doi.org/10.36922/IJOCTA025290127
22. Atangana A, Baleanu D. New fractional derivatives with nonlocal and non-singular kernel: theory and application to heat transfer model. *arXiv preprint arXiv:160203408.* 2016. https://www.doi.org/10.48550/arXiv.1602.03408
23. Raza N, Raza A, Chahlaoui Y, Gomez-Aguilar JF. Numerical analysis of HPV and its association with cervical cancer using Atangana–Baleanu fractional derivative. *Model Earth Syst Environ.* 2025;11(1):60. https://www.doi.org/10.1007/s40808-024-02243-5
24. Khan NA, Ali M, Ayaz M, Khan NA. Design of an operational matrix method based on Haar wavelets and evolutionary algorithm for time-fractional advection–diffusion equations. *Open Eng.* 2025;15(1):20250142. https://www.doi.org/10.1515/eng-2025-0142
25. Atangana A. *Derivative with a New Parameter: Theory, Methods and Applications.* Academic Press; 2015.
26. Abuzeid OM. A novel hereditary viscoelastic Fractional-Fractal creep model for the contact of rough surfaces: Maxwell medium. *Ain Shams Eng J.* 2025;16(8):103458. https://www.doi.org/10.1016/j.asej.2025.103458
27. Murtaza S, Ismail EAA, Awwad FA, et al. Parametric simulations of fractal-fractional non-linear viscoelastic fluid model with finite difference scheme. *AIP Adv.* 2024;14(4):045220. https://www.doi.org/10.1063/5.0180414
28. Priya P, Sabarmathi A, Akgül A, Hassani MK. Novel adaptive control approach to fractal fractional order deforestation model and its impact on soil erosion. *Sci Rep.* 2024;14(1):27996. https://www.doi.org/10.1038/s41598-024-74352-1
29. Shah MI, Hassan EI, Ali A, Muhyi A, Ahmed WE, Aldwoah K. Controlling worm propagation in wireless sensor networks: through fractal-fractional mathematical perspectives. *PLoS One.* 2025;20(11):e0335556. https://www.doi.org/10.1371/journal.pone.0335556
30. Uçar E, Uçar S, Evirgen F, Özdemir N. Investigation of E-cigarette smoking model with mittag-leffler kernel. *Fund Comput Decis Sci.* 2021;46(1):97–109. https://www.doi.org/10.2478/fcds-2021-0007
31. Abdeljawad T, Sher M, Shah K, et al. Analysis of a class of fractal hybrid fractional differential equation with application to a biological model. *Sci Rep.* 2024;14(1):18937. https://www.doi.org/10.1038/s41598-024-67158-8
32. Uçar E, Uçar S, Evirgen F, Özdemir N. A fractional SAIDR model in the frame of Atangana–Baleanu derivative. *Fractal Fract.* 2021;5(2):32. https://www.doi.org/10.3390/fractalfract5020032
33. Alhazmi M, Aljohani AF, Taha NE, Abdel-Khalek S, Bayram M, Saber S. Application of a fractal fractional operator to nonlinear glucose–insulin systems: adomian decomposition solutions. *Comput Biol Med.* 2025;196:110453. https://www.doi.org/10.1016/j.compbiomed.2025.110453
34. Bala B, Behal S. AI techniques for IoT-based DDoS attack detection: taxonomies, comprehensive review and research challenges. *Comput Sci Rev.* 2024;52:100631. https://www.doi.org/10.1016/j.cosrev.2024.100631
35. Khan ZU, ur Rahman M, Arfan M, Waseem, Boulaaras S. The artificial neural network approach for the transmission of malicious codes in wireless sensor networks with Caputo derivative. *Int J Numer Model Electron Netw Devices Fields.* 2024;37(3):e3256. https://www.doi.org/10.1002/jnm.3256
36. Aychluh M, Suthar DL, Cesarano C, Purohit SD. Modeling and analysis of the dynamics of an excessive gambling problem with modified fractional operator. *Int J Optim Control Theor Appl.* 2025;15(3):407–425. https://www.doi.org/10.36922/ijocta.7096
37. Zaeem RA, Chang C-Y, Khan MP, Shoaib M, Shu C-M, Raja MAZ. Machine learning solutions with deep multilayer exogenous networks for distributed denial of service attacks model on net-

worked resources in critical infrastructure. *Eng Appl Artif Intel.* 2026;163:112872. https://www.doi.org/10.1016/j.engappai.2025.112872

38. Rao YS, Keshri AK, Mishra BK, Panda TC. Distributed denial of service attack on targeted resources in a computer network for critical infrastructure: a differential e-epidemic model. *Physica A Stat Mech Appl.* 2020;540:123240. https://www.doi.org/10.1016/j.physa.2019.123240
39. Pham TH, Hoang TM. A simple approach to the study of global asymptotic stability of some modified continuous-time epidemiological models for distributed denial of service attacks. *Ann Univ Craiova Math Comput Sci Ser.* 2025;52(1):81–100. https://www.doi.org/10.52846/ami.v52i1.1925
40. Atangana A, Qureshi S. Modeling attractors of chaotic dynamical systems with fractal–fractional operators. *Chaos Solitons Fractals.* 2019;123:320–337. https://www.doi.org/10.1016/j.chaos.2019.04.020

Mumtaz Ali *is a Lecturer at Balochistan University of Engineering and Technology, Khuzdar, Balochistan, Pakistan. He is currently pursuing a Ph.D. in Applied Mathematics at the University of Karachi, Pakistan, and is on a one-year research visit at Universiti Tekenologi PETRONAS, Malaysia. His research interests include fractional differential equations, wavelet-based numerical methods, mathematical modeling, and numerical analysis, with applications to scientific and engineering problems. He has published four research papers in peer-reviewed journals.*
https://orcid.org/0009-0004-3805-6808

Nazreen Waeleh *is a Lecturer at Universiti Teknikal Malaysia Melaka, Malaysia. She received her B.Sc. (Hons) degree in Mathematics, M.Sc. degree in Numerical Analysis, and Ph.D. degree in Biomedical Engineering from Universiti Putra Malaysia,Malaysia. Her research interests are in numerical analysis and computational methods for differential equations, with recent work in medical imaging and signal processing.*
https://orcid.org/0000-0002-6518-4539

Nooraini Zainuddin *is a Lecturer at Universiti Teknologi PETRONAS. She received her bachelor's degree in Mathematics, her master's degree in Numerical Analysis, and her Ph.D. degree in Applied Mathematics from Universiti Putra Malaysia in 2009, 2012, and 2017, respectively. Her research interests include numerical methods for differential equations and their applications.*
https://orcid.org/0000-0002-0624-0721

Hanita Daud *is an Associate Professor at Universiti Teknologi PETRONAS. She received her Ph.D. in Statistics from Universiti Teknologi PETRONAS in 2013, Master of Science in Information Technology from Universiti Kebangsaan Malaysia in 2001, and Bachelor of Science in Statistics from Macquarie University, Sydney, Australia in 1989. Her research interests are in simulation and optimization, artificial intelligence, and statistical/mathematical modelling. She has been in academic for more than 30 years with more than 200 publications in her field of interest.*
https://orcid.org/0000-003-1377-4606

Rahimah Jusoh *is a Senior Lecturer at the Centre for Mathematical Sciences, Universiti Malaysia Pahang Al-Sultan Abdullah. She received her B.Sc. (Industrial Mathematics) and M.Sc. (Mathematics) degrees from Universiti Teknologi Malaysia in 2007 and 2009, respectively. She completed her PhD in Applied Mathematics at Universiti Kebangsaan Malaysia in 2019. Her research interests include boundary layer flow, fluid dynamics, and mathematical modelling.*
https://orcid.org/0000-0002-7049-9121